U.S. DEPARTMENT OF COMMERCE
National Technical Information Service

PB-264 203

Effects of Temperature and Pressure on Particle Collection Mechanisms Theoretical Review

A P T, Inc, San Diego, Calif

Prepared for

Industrial Environmental Research Lab, Research Triangle Park, N C

Jan 77

PB 264 203

PA [illegible]

EPA-600/7-77-002
January 1977

EFFECTS OF TEMPERATURE AND PRESSURE ON PARTICLE COLLECTION MECHANISMS:

Theoretical Review

Interagency
Energy-Environment
Research and Development
Program Report

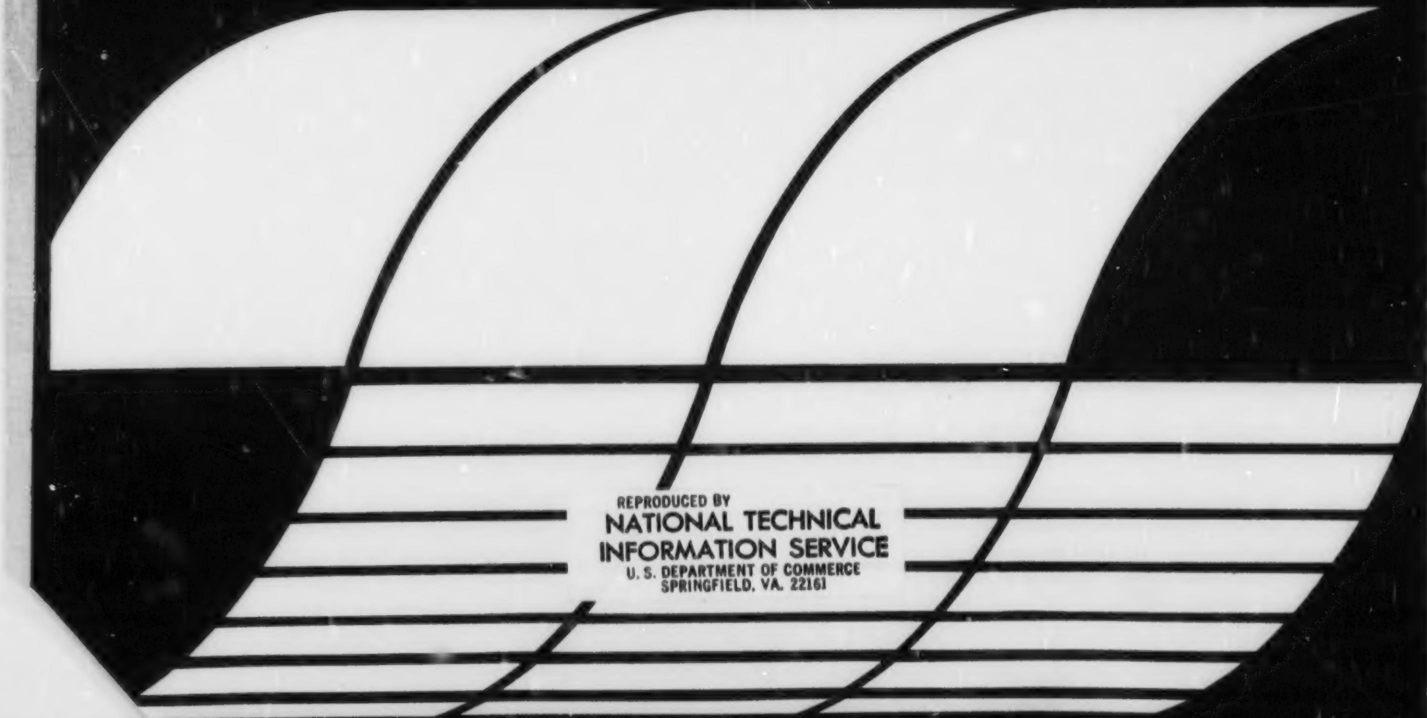

REPRODUCED BY
NATIONAL TECHNICAL
INFORMATION SERVICE
U. S. DEPARTMENT OF COMMERCE
SPRINGFIELD, VA. 22161

TECHNICAL REPORT DATA
(Please read Instructions on the reverse before completing)

1. REPORT NO. EPA-600/7-77-002	2.	3. RECIPIENT'S ACCESSION NO.
4. TITLE AND SUBTITLE Effects of Temperature and Pressure on Particle Collection Mechanisms: Theoretical Review		5. REPORT DATE January 1977
		6. PERFORMING ORGANIZATION CODE
7. AUTHOR(S) Seymour Calvert and Richard Parker		8. PERFORMING ORGANIZATION REPORT NO.
9. PERFORMING ORGANIZATION NAME AND ADDRESS A. P. T., Inc. 4901 Morena Boulevard, Suite 402 San Diego, California 92117		10. PROGRAM ELEMENT NO. EHE623A
		11. CONTRACT/GRANT NO. 68-02-2137
12. SPONSORING AGENCY NAME AND ADDRESS EPA, Office of Research and Development Industrial Environmental Research Laboratory Research Triangle Park, NC 27711		13. TYPE OF REPORT AND PERIOD COVERED Final; 12/75-9/76
		14. SPONSORING AGENCY CODE EPA/600/13

15. SUPPLEMENTARY NOTES IERL-RTP Project Officer for this report is D.C. Drehmel, 919/549-8411 Ext 2925, Mail Drop 62.

16. ABSTRACT The report is a critical review and evaluation of the mechanics of aerosols at high temperatures and pressures. It discusses equations and models used to predict particle behavior at normal conditions, with regard to their applicability at high temperatures and pressures. It discusses available experimental data, concluding that the data are inadequate to confirm the projections of aerosol mechanics at high temperatures and pressures. It presents a few examples of the effects of high temperature and pressure on the collection efficiency and power requirement of typical collection devices. It concludes, generally, that particle collection at high temperatures and pressures will be much more difficult and expensive than collection of similar particles at low temperatures and pressures.

17. KEY WORDS AND DOCUMENT ANALYSIS

a. DESCRIPTORS	b. IDENTIFIERS/OPEN ENDED TERMS	c. COSATI Field/Group
Air Pollution	Air Pollution Control	13B
Dust	Stationary Sources	11G
Aerosols	Particulate	07D
Collection		14A
Temperature		
Pressure		

18. DISTRIBUTION STATEMENT Unlimited	19. SECURITY CLASS *(This Report)* Unclassified	21. NO. OF PAGES 96
	20. SECURITY CLASS *(This page)* Unclassified	22. PRICE

EPA Form 2220-1 (9-73)

EPA-600/7-77-002
January 1977

EFFECTS OF TEMPERATURE AND PRESSURE ON PARTICLE COLLECTION MECHANISMS: THEORETICAL REVIEW

by

Seymour Calvert and Richard Parker

A.P.T., Inc.
4901 Morena Boulevard, Suite 402
San Diego, California 92117

Contract No. 68-02-2137
Program Element No. EHE623A

EPA Project Officer: Dennis C. Drehmel

Industrial Environmental Research Laboratory
Office of Energy, Minerals, and Industry
Research Triangle Park, NC 27711

Prepared for

U.S. ENVIRONMENTAL PROTECTION AGENCY
Office of Research and Development
Washington, DC 20460

ABSTRACT

A critical review and evaluation of the mechanics of aerosols at high temperatures and pressures are presented. The equations and models used to predict particle behavior at normal conditions are discussed with regard to their applicability at high temperatures and pressures. The available experimental data are discussed and found to be inadequate to confirm the projections of aerosol mechanics at high temperatures and pressures. A few examples of the effects of high temperature and pressure on the collection efficiency and power requirement of typical collection devices are presented. In general, particle collection at high temperatures and pressures will be much more difficult and expensive than the collection of similar particles at low temperatures and pressures.

This report was submitted in partial fulfillment of contract number 68-02-2137 by Air Pollution Technology, Inc. under the sponsorship of the U.S. Environmental Protection Agency. This report covers the period December 5, 1975 to September 10, 1976, and work was completed as of September 30, 1976.

Preceding page blank

CONTENTS

Page

Abstract. iii
List of Figures v
List of Tables. vii
List of Symbols viii
Acknowledgement xii

Sections

Summary and Conclusions 1
Introduction. 6
Fundamental Considerations. 13
Collection Mechanisms 26
Properties. 56
Example Applications. 69
Bibliography. 79

LIST OF FIGURES

No. Page

1 Collection efficiency of a nucleopore filter as a function of absolute pressure. 9

2 The effect of temperature and pressure on the kinematic viscosity of air. 17

3 Validity of Stokes' law at high temperature and pressure. 18

4 Validity of Stokes' law at high temperature and pressure. 19

5 The effect of temperature and pressure on the ratio of the Cunningham slip correction factor to the dynamic viscosity of air 20

6a The effects of temperature and pressure on the particle inertial relaxation time 28

6b The effects of temperature and pressure on the particle inertial relaxation time 29

7 The effect of interception on the particle collection efficiency by a circular cylinder. . . . 31

8 The effects of temperature and pressure on particle diffusivity. 33

9 Thermal deposition velocity as a function of temperature and pressure. 42

10 The effect of pressure on the diffusiophoretic deposition velocity 45

11 Thermal coagulation of particles at high temperature and pressure. 50

12 Turbulent agglomeration tendency of particles at high temperature and pressure. 53

13 Sonic agglomeration of particles at high temperature and pressure. 55

14 Experimental and theoretical viscosity versus temperature curves for air. 58

15 Gas viscosity versus temperature. 59

No. Page

16 Mean free path of air molecules as a function of temperature and pressure 61

17 Specific heat as a function of temperature for air at 1 atm. 64

18 The effect of temperature on the thermal conductivity of air at 1 atm pressure 65

19 Molecular diffusivity of water vapor in air as a function of temperature. 67

20 The thermal expansion of silica brick at high temperatures 68

21 Flow work (specific power) for impaction from a round jet as a function of temperature and pressure. 70

22 The effects of high temperature and pressure on the collection efficiency of a high efficiency cyclone. 73

23 The specific power requirements for a cyclone as a function of temperature and pressure 75

24 The effects of high temperature and pressure on the collection efficiency of a fiber bed 76

25 The effects of high temperature and pressure on the inertial collection efficiency of a packed bed. 78

LIST OF TABLES

No. Page

1 Brownian Diffusion Reynolds Numbers for a 0.002 μm Diameter Particle at Various Temperatures and Pressures. 34

2 Numbers of Charges Acquired by a Particle: a) Ion Bombardment; b) Ion Diffusion, 27°C; c) Ion Diffusion, 1,100°C 39

3 The Effects of High Pressure and Drop Diameter on the Growth of Drops by Condensation. 47

4 Effect of Temperature on the Agglomeration of Charged Particles. 51

LIST OF SYMBOLS

A - dimensionless constant in equation (14)

A_d - deposition area, m^2

B - dimensionless constant in equation (14)

B_i - ion mobility, s/kg

B_p - particle mobility, s/kg

$\bar{c}$ - root mean square molecular velocity, m/s

C_m - isothermal slip coefficient, dimensionless

C_t - temperature jump coefficient, dimensionless

C' - Cunningham slip correction factor, dimensionless

C_D - drag coefficient, dimensionless

C_G - velocity of sound in gas, m/s

d_c - collector diameter, m

d_d - drop diameter, m

d_o - initial drop diameter, m

d_p - particle diameter, m

D_c - cyclone diameter, m

D_p - particle diffusivity, m^2/s

D_t - turbulent diffusivity, m^2/s

D_{VG} - molecular diffusivity, m^2/s

e - unit electronic charge, e.s.u.

e_o - energy dissipation rate, m^2/s^3

E - collection efficiency, fraction

E_c - charging electric field strength, V/m

E_o - actual applied electric field strength, V/m

E_p - effective precipitating electric field strength, V/m

F_r - gas resistance force, kg-m/s^2
g - acceleration of gravity, m/s^2
H - magnetic field strength, A/m
k - Boltzmann's constant, J/°K
k_G - gas thermal conductivity, J/m-s-°K
k_p - particle thermal conductivity, J/m-s-°K
k_t - thermal conductivity, J/m-s-°K
K_a - sonic agglomeration constant, m^3/s
K_o - coagulation constant, m^3/s
K_p - inertial impaction parameter, dimensionless
M_G - molecular weight of gas, g/gmole
M_s - molecular weight of surface molecules, g/gmole
M_v - molecular weight of vapor, g/gmole
n - vortex exponent for cyclone, dimensionless
N_i - ion number concentration, m^{-3}
N_{Kn} - Knudsen number, dimensionless
N_p - particle number concentration, m^{-3}
N_{Pe} - Peclet number, dimensionless
N_{Re} - Reynolds number, dimensionless
N_{Ref} - fiber Reynolds Number, dimensionless
N_{Sc} - Schmidt number, dimensionless
p_∞ - vapor pressure in gas stream, Pa
p_{BM} - mean partial pressure of non-transferring gas, Pa
p_o - vapor pressure at drop surface, Pa
p_G - gas partial pressure, Pa
p_v - vapor partial pressure, Pa
P - absolute pressure, Pa

Pt - penetration, fraction

q_p - particle charge, C

q_s - saturation charge, C

Q_G - gas volumetric flow rate, m³/s

Q_x - heat flux in "x" direction, J/m²-s

$\mathcal{R}$ - universal gas constant, J/gmole-°K

t - time, s

T, T_{abs} - absolute temperature, °K

T_g - temperature of incident gas molecules, °K

T_r - temperature of reflected molecules, °K

T_s - surface temperature, °K

u_c - centrifugal deposition velocity, m/s

u_d - deposition velocity, m/s

$\overline{u}_{BD}$ - average Brownian diffusion velocity, m/s

u_D - diffusiophoretic deposition velocity, m/s

u_e - electrical migration velocity, m/s

u_f - superficial gas velocity, m/s

u_G - gas velocity, m/s

u_m - magnetic deposition velocity, m/s

u_r - relative particle-gas velocity, m/s

u_s - gravitational settling velocity, m/s

u_t - thermophoretic deposition velocity, m/s

Z - depth of granular bed, m

Greek

α_m - fraction of diffusely reflected molecules, dimensionless

α_t - thermal accommodation coefficient, dimensionless

β - proportionality constant in equation (49), dimensionless

γ - ratio of specific heats, dimensionless

δ - boundary layer thickness, m

$\Delta\eta_i$ - interception collection efficiency, fraction

ε - dielectric constant, dimensionless

ε_o - permittivity constant, $C^2/N\text{-}m^2$

η_s - single fiber collection efficiency, fraction

λ - mean free path of gas molecules, m

μ_G - gas absolute viscosity, kg/m-s

μ_o - permeability constant, V-s/A-m

ν_G - gas kinematic viscosity, m^2/s

ρ_G - gas density, kg/m^3

ρ_L - liquid drop density, kg/m^3

ρ_p - particle density, kg/m^3

Ψ - modified impaction parameter in equation (54), dimensionless

τ - relaxation time, s

τ_G - frictional shear stress in a gas, N/m^2

ACKNOWLEDGEMENT

A.P.T., Inc. wishes to express its appreciation for excellent technical coordination and for very helpful assistance in support of our technical effort to Dr. Leslie Sparks of the E.P.A. and Dr. Dennis Drehmel, E.P.A. Project Officer.

SUMMARY AND CONCLUSIONS

The objective of this study was to conduct a critical review and evaluation of all available information concerned with the mechanics of aerosols at high temperature and/or high pressure. The specific goal was to determine the availability, adequacy, and useful ranges of the models, equations, and experimental data which may be used to predict the effects of temperature and pressure on particle behavior.

The literature review turned up a number of reports of studies dealing with the development of high temperature and pressure particle collection equipment. Most of these studies were concerned with operational problems and overall pressure drops and collection efficiencies of the equipment when operating at high temperatures and pressures. They were not concerned with the effects of temperature and pressure on the fundamental particle collection mechanisms.

There have been a few studies concerned with the effects of temperature and pressure on the basic collection mechanisms. In general, these studies have used accepted theory for the mechanics of aerosols at low temperature and pressure and extrapolated it to high temperatures and pressures by adjusting the gas properties. They did not discuss the validity of this extrapolation, other than to note that experimental verification is lacking. Although experimental data were presented in some studies, they were not sufficient to test the theory at high temperature and pressure. Generally the experimental results have been in qualitative agreement with theoretical predictions.

The work presented by previous authors has been reviewed and evaluated in the present study. Our primary intent has been to identify the regions of temperature, pressure, and particle size where existing theoretical and/or experimental information is either adequate or inadequate.

REVIEW

For most particle collection mechanisms, the collection efficiency, E, is a function of the fluid resistance force, which is proportional to the ratio of the Cunningham slip correction factor, C', to the gas viscosity, μ_G. The Cunningham correction factor is a function of the particle diameter, gas temperature, pressure, and viscosity. It increases with temperature and decreases with pressure and particle diameter. The gas viscosity increases with temperature and pressure, although the effect of pressure is negligible below about 20 atm.

Therefore, for particles greater than a few tenths of a micron in diameter, particle collection efficiency decreases as temperature and pressure increase. For very small particles, particle collection efficiency will increase with temperature but will decrease with pressure.

The above conclusions are based on available theoretical models. The data needed to confirm the extrapolation of the theory of aerosol mechanics to high temperatures and pressures are not presently available.

EVALUATION

The effects of high temperature and pressure on the properties of gases and particles have been studied theoretically and experimentally. Gas densities, viscosities, molecular mean free paths, thermal conductivities, and molecular diffusivities may be predicted as a function of temperature and pressure with good accuracy. The theories have been verified by experimental data. There should be no difficulty in predicting the properties of gases (or gas mixtures) at high temperature and pressure.

The effects of high temperature on particle properties generally are less important, and less well defined. The most important particle properties are: density, thermal conductivity, coefficient of thermal expansion, and dielectric constant. The density, thermal conductivity, and dielectric constant usually are considered independent of temperature, although data to confirm this for fly ash at extreme temperatures (over 1,000°C) have not been found. The coefficient of thermal expansion of refractory material (such as silica) increases with temperature, but is too small to be of much significance (approximately 1% increase in length as temperature increases from 0°C to 1,000°C.)

The major difficulty in extending the theory of aerosol mechanics to high temperature is to determine what form of the Cunningham correction factor, C', is applicable. The Cunningham correction factor is an empirical factor which was used to match experimental data at room temperature and very low pressure. From theoretical arguments, the empirical constants in "C'" [as presented in equation (14)] are functions of the momentum and energy accommodation of the gas molecules impinging on the particle surface. That is, they depend on the efficiency with which the molecular momentum and energy are transferred to the particle.

Available theory and experiment indicate that the molecular momentum and energy accommodation coefficients decrease with increasing temperature. This would mean that the gas (molecule) resistance to the particle's motion would decrease more with temperature than would be predicted using the low temperature form for "C'" [equation (12)]. The magnitude of the resulting decrease in the drag force could be as much as 50% for submicron particles. The drag force on large particles would be affected much less.

The above discussion is based on theory and experiment for very pure gases and surfaces. The effect of temperature on the accommodation coefficient may be much different for actual effluent gases and fly ash particles.

Gas pressure has been found to have no effect on the accommodation coefficient, and thus would not be expected to influence the applicable form of "C'". High pressures, however, decrease the molecular mean free path and increase the interaction between molecules. At pressures greater than about 20 atm (and at room temperature), the gas begins to depart from the perfect gas law. The pressure then has an influence on the transport properties of the gas (that is, viscosity, thermal conductivity, and molecular diffusivity). There should be no problem determining the effects of high pressure on the particle collection mechanisms, as long as the effects of pressure on the gas are considered.

At high temperatures, the influence of pressure on the gas properties is decreased greatly. For example, at 1,100°C, the gas viscosity is effectively independent of pressures up to more than 300 atm.

Another uncertainty in the collection of particles at high temperature is in the magnitude of the thermal force. The thermal force is a function of the energy accommodation of the molecules at the particle surface. It is expected, therefore, that the thermal force would be less than predicted at high temperatures because of the less efficient energy and momentum transfer from the molecule to the particle. Experimental verification of this prediction is needed.

CONCLUSIONS

The theory and experimental data needed for predicting the effects of temperature and pressure on the important gas properties are available and adequate. The effects of temperature and pressure on particle properties are less important, and less well documented. Data on the thermal conductivity and dielectric constant for fly ash particles at extreme temperatures (greater than 1,000°C) could not be found.

The major uncertainty in applying the theory of aerosol mechanics at high temperatures and pressures is in properly predicting the gas resistance force on the particle. High temperatures are expected to decrease the accommodation coefficients between the molecules and the particle, and thereby decrease the gas resistance relative to low temperature theory. This effect would be most important for small particles and low pressures, and would have its largest influence on the collection of particles by Brownian diffusion.

However, the collection of particles larger than a few tenths of a micron in diameter is expected to be much more difficult at higher temperatures. High pressures further aggravate the problem.

Experimental measurements of the drag force and particle diffusivity at high temperature and pressure are needed to verify the above predictions, and to modify existing theory for application to high temperature and pressure particle collection.

It is unlikely that a new particle collection device will be devised which can collect particles at high temperature and pressure more efficiently than at standard conditions. It is more probable that high temperature and pressure particle cleanup will have to be achieved by equipment (such as cyclones, metal or ceramic filters, granular beds) operating at higher costs (larger power consumption) than would be needed for operation at standard conditions.

INTRODUCTION

In many industrial situations, the life of critical components, such as turbine blades and heat exchanger tubes, is limited by the extent of erosion and corrosion damage that results from the presence of particulate matter in the process gas streams. It is often economically desirable, therefore, to remove the particulate matter while the gas is still at a high temperature and pressure, prior to passing the gas through heat exchangers, gas turbines, or other critical equipment.

Although high temperature and pressure particle collection has been under investigation for over thirty years, no fully satisfactory solution to the problem has been achieved. This is in contrast to the great advances that have been made in the collection of particulate matter at low and intermediate temperatures. To better understand, develop, and evaluate particle collection equipment for high temperature and pressure gas cleaning, it is important to obtain a firm understanding of the effects of high temperature and pressure on the basic particle collection mechanisms.

The basic mechanisms by which particles can be removed from gas streams have been discussed by many authors, including: Fuchs (1964), Green and Lane (1964), and Hidy and Brock (1970). The theory presented by these authors has been developed for application to moderate temperature and pressure particle collection. In order to extrapolate this theory to high temperatures and pressures, it is not sufficient merely to insert values for the gas and particle properties at high temperature and pressure. It also is necessary to look at the fundamental laws and assumptions on which the theory is based, and thereby to determine whether or not the theory is valid at high temperatures and pressures.

REVIEW OF PREVIOUS WORK

Fundamental investigations of the mechanics of aerosols at high temperatures and pressures are very scarce. There have been few theoretical studies, and there have been even fewer experimental studies to evaluate the theory. Most of the high temperature and pressure experimental studies reported in the literature have dealt with the operational characteristics of specific particle collection equipment. Only general, qualitative comparisons between theory and experiment were made.

Silverman (1955) discussed the technical aspects of high temperature gas cleaning for steel making processes, and presented some results of attempts to use inertial cleaners, wet cleaners, filtration units, and electrostatic precipitators at moderately high temperatures (250°C to 600°C). He presented the general theory describing particle collection mechanisms in fiber filtration, and he used it qualitatively to explain some of the experimental results. In general, he found that particle collection is more difficult at high temperature, and that inertial impaction and diffusion are the most important mechanisms for high temperature filtration.

Thring and Strauss (1963) predicted the effects of high temperature on particle collection mechanisms for temperatures up to 1,600°C. They also presented the results of some experimental studies for fiber filters up to 980°C, and for pebble bed filters and electrostatic precipitators up to 650°C. Their theoretical study considered electrical migration, inertial impaction, direct interception, diffusion, and thermal precipitation. The available experimental data were for particle collection devices involving complicated combinations of collection mechanisms, and therefore only a qualitative comparison between experiment and theory could be made. Some of their results are reported by Strauss (1966).

To determine the effects of ash deposition on turbine blades at high temperature, Morley and Wisdom (1964) studied the deposition of ash particles onto a cylinder placed in the outlet gas stream of a brown coal combustor (700°C). They made no attempt to compare the amount of deposition with theory. They tried cooling the cylinder (400°C) and did notice an increase in deposition. This was attributed to thermal deposition.

Strauss and Lancaster (1968) calculated the effects of high temperature (800°C) and high pressure (100 atm) on the fundamental particle collection mechanisms, and concluded that the collection efficiencies of all cleaning processes will be reduced under these conditions. They considered electrostatic precipitation to be the most promising method for collecting particulate matter at high temperature and pressure. Their theoretical study included the effects of temperature and pressure on gas properties, particle properties, and the important collection parameters. They discussed some of the earlier experimental work but were unable to make any quantitative comparisons with theory.

Gussman and Sacco (1970) investigated the hazards that might arise from the presence of aerosols in a high pressure environment. They were interested in the effects of pressure on the formation and behavior of aerosols in the atmosphere of diving vessels (to 1,000 ft). They were concerned with an oxygen-helium atmosphere and pressures up to 34 atm. They considered various air cleaning mechanisms and did experimental work with electrostatic precipitation at this pressure. Their work is of limited value to the present study because they were only interested in particles smaller than 0.1 μm.

Spurný et al. (1971) conducted a theoretical study of the effect of temperature (to 1,500°C) and pressure (to 50 atm) on the collection efficiency of a nucleopore type filter. They considered the collection mechanisms of inertial impaction, direct interception, and diffusion. They also conducted an experimental study of the effect of pressure on the collection efficiency. Their results are shown in Figure 1. They were concerned primarily with low (vacuum) pressure, but their high pressure data do confirm their prediction that the efficiency is not affected greatly by high pressures.

Calvert et al. (1972) investigated the effects of pressure and temperature on the collection of particles in wet scrubbers. Their study was limited to scrubber operating conditions of 1 to

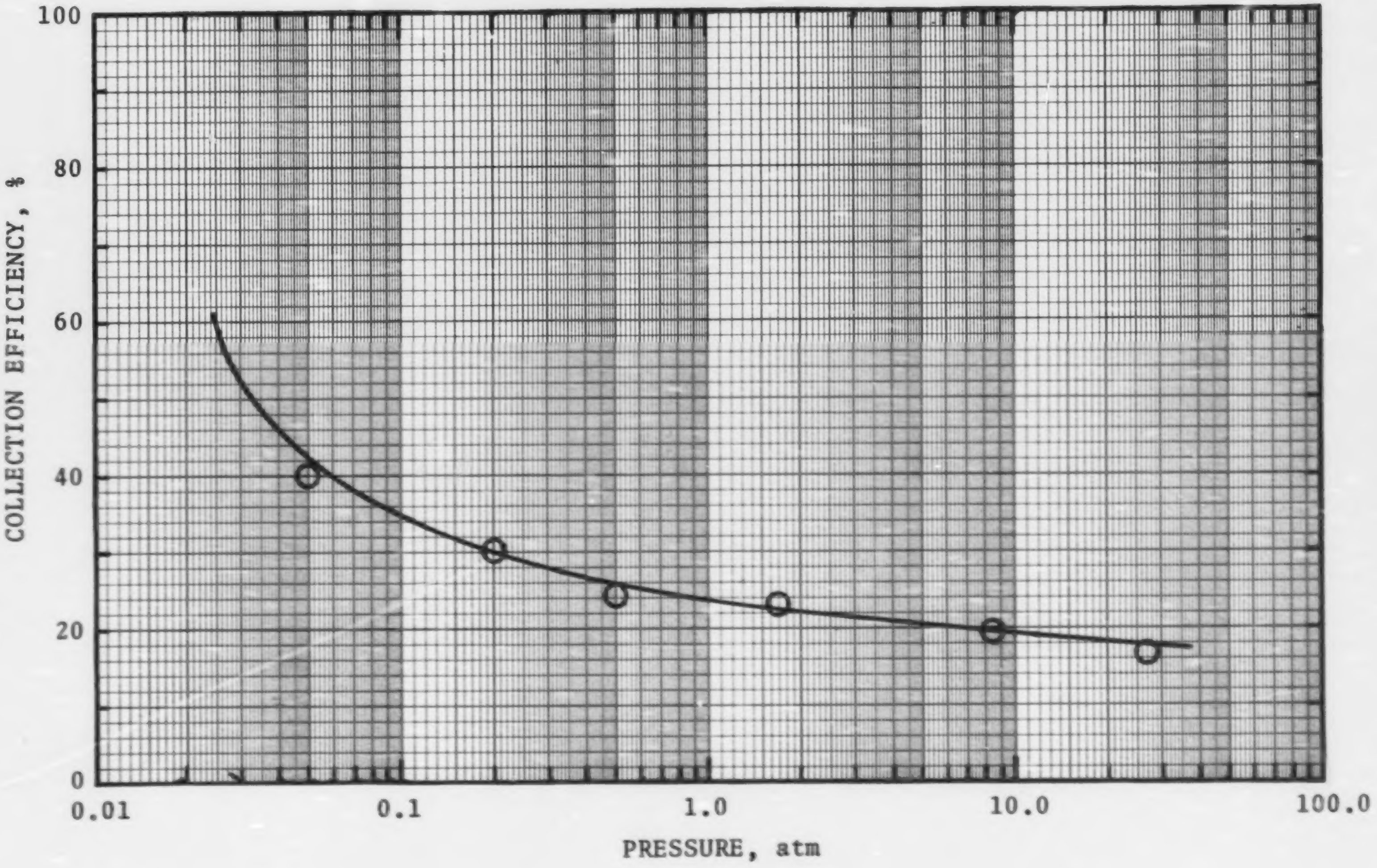

Figure 1. Collection efficiency of a nucleopore filter as a function of absolute pressure. From Spurný, et al. (1971)

10 atm pressure and temperatures from 0°C to 100°C. The collection mechanisms that were considered included: inertial impaction, direct interception, diffusion, thermophoresis, electrical migration, centrifugal deposition, and diffusiophoresis. No experimental data were presented.

Kornberg (1973) experimentally investigated the high temperature (to about 450°C) filtration of particles by diffusion, and compared his results with theory. He concluded that current diffusional filtration theory is adequate for predicting filter efficiencies at high temperature. This work is discussed in more detail in a later section.

A fairly recent study, reported by Rao et al. (1975), presents a review of the earlier theoretical work and also discusses some collection mechanisms and particle agglomeration methods which were not considered in previous studies. In general, particle collection efficiencies for all mechanisms were predicted to decrease as temperature and pressure increase for particles larger than a few tenths of a micron in diameter. No experimental data were presented.

The high temperature and pressure particle collection models described in the above studies were based on projections of the available theory to high temperature and pressure conditions. Basically, this involved adjusting the gas properties to their high temperature and pressure values. There has been no critical review aimed at determining the uncertainties and applicability of this theory at high temperatures and pressures. Also no experimental data have been found which could be used to confirm the validity of extrapolating the theory of the mechanics of aerosols to high temperatures and pressures.

In addition to the above studies dealing with the mechanics of aerosols at high temperature and pressure, there have been a number of experimental investigations concerned with high temperature and pressure particle collecting equipment. These studies do not present sufficient data to evaluate the theory of the basic particle collection mechanisms.

Experimental measurements of the efficiency of cyclone separators at high temperatures and pressures have been reported by Parent (1946) and by Yellott and Broadley (1955). Parent considered temperatures up to 650°C. The collection efficiency was found to drop off as the temperature was raised, for a constant pressure drop through the cyclone. To maintain a constant efficiency at a higher temperature (increasing from 25°C to 550°C), approximately 2½ times the pressure drop was required.

Yellott and Broadley (1955) considered the efficiency and pressure drop of cyclones operating at temperatures up to 700°C and pressures to 5 atm. They also found that efficiency decreased with increasing temperature. To maintain a 95% efficiency as the temperature increased from 25°C to 550°C, over three times the pressure drop was required.

The filtration of hot gases has been studied by many authors, including: Snyder and Pring (1955), Billings, et al. (1955, 1958a, 1958b, 1960), First, et al. (1956), Kane, et al. (1960), Spaite, et al. (1961), and Lundgren and Gunderson (1976). Snyder and Pring were concerned with the operational and design considerations for the filtration of hot gases. Billings, et al. performed pilot-plant and full scale performance tests of slag-wool filters operating at atmospheric pressure and temperatures over 500°C. They were concerned primarily with the operational problems of the slag-wool filter. Their data did, however, confirm that the filter efficiency decreases with increasing temperature.

First, et al. (1956) measured the efficiency of a ceramic fiber filter at temperatures up to 800°C, for various filter depths, fiber diameters, and face velocities. In all cases the collection efficiency decreased with increasing temperature as predicted, qualitatively, from impaction theory. Kane, et al. (1960) reported similar tests on a ceramic fiber filter at a temperature of about 1,000°C. They were concerned with pressure drop and dust loading, and did not measure the efficiency as a function of temperature. Spaite, et al. (1961) discuss the operational problems and applications of high temperature filtration.

Lundgren and Gunderson (1976) investigated a high-purity "microquartz" fiber filter medium at temperatures up to 540°C (1,000°F). Qualitative agreement between theory and experiment was obtained, however the theoretical penetrations were only within two orders of magnitude of the experimental penetrations. More work is being done to improve the theory.

High temperature and pressure electrostatic precipitation has been studied by many authors over the past thirty years, including: Koller and Fremont (1950), Thomas and Wong (1958), Shale, et al. (1963, 1964, 1965, 1967, 1969), Robinson (1967, 1969), and Brown and Walker (1971). These studies dealt primarily with the problems of corona generation and the current-voltage characteristics of electrostatic precipitators at high temperature and pressure. Although Brown and Walker (1971) demonstrated the feasibility of electrostatic precipitation at a temperature of over 900°C, and at a pressure of 7 atm, the particle migration velocity was much lower than normal for a given applied voltage. This was attributed to the larger gas viscosity at high temperature.

In the following sections, the equations and models for predicting the behavior of particles at high temperature and pressure are presented and critically reviewed. Emphasis has been placed on identifying the regions of temperature, pressure, and particle size where existing theoretical information is inadequate.

In the final section, a few examples of the effects of high temperature and pressure on particle collection devices are presented. The available experimental data are not sufficient to verify the theory for these examples.

FUNDAMENTAL CONSIDERATIONS

The models and equations describing particle collection mechanisms have some fundamental theoretical considerations in common. The most important of these is the description of the drag or resistance force which is exerted on a particle by the gas, when the particle moves relative to the gas stream. In particle collection theory, the motion of the particle relative to the gas stream generally is characterized by a deposition velocity, u_d.

In most particle collection equipment, the flow is turbulent and it can be assumed that there is complete mixing of the suspended particles. In this case, the deposition velocity can be related to the particle collection efficiency, E, through the particle penetration, Pt, as follows:

$$Pt = 1 - E = \exp\left(-\frac{u_d A_d}{Q_G}\right) \qquad (1)$$

where "A_d" is the deposition area, and "Q_G" is the volumetric flow rate of the gas. For any collection device, the penetration is defined as:

$$Pt = \frac{\text{Outlet concentration}}{\text{Inlet concentration}} \qquad (2)$$

The deposition velocity for any collection mechanism depends on the force balance between the driving force (deposition force) and the resistance force of the gas. In this section, the basic equations describing the gas resistance force will be reviewed with regard to their application to high temperature and pressure particle collection. The specific driving force for each collection mechanism will be reviewed in a subsequent section.

STOKES' LAW

The major difference between the collection of particles at normal conditions and at high temperature and pressure is in the resistance force of the gas. For a rigid, spherical particle moving through a continuous, viscous gas at constant relative velocity, and for negligible inertial effects arising from the gas being displaced by the particle, the resistance force, F_r, is given by Stokes' law:

$$F_r = - 3\pi \mu_G d_p u_r \tag{3}$$

where "μ_G" is the gas viscosity, "d_p" is the particle diameter, and "u_r" is the relative velocity between the particle and the gas. The negative sign indicates that the drag force is opposite to the direction of motion of the particle.

If the mean free path of the gas molecules (related to the effective spacing between the gas molecules) is not negligible with respect to the particle diameter, the particle no longer sees the gas as a continuous fluid but rather as a finite number of discrete molecules. In this case, equation (3) usually is modified by an empirical correction factor, C', so that the modified Stokes' law becomes:

$$F_r = \frac{- 3\pi \mu_G d_p u_r}{C'} \tag{4}$$

The correction factor, C', is often referred to as the "Cunningham slip correction factor" because of the pioneering work of Cunningham (1910). The slip correction factor will be discussed in more detail later in this section.

Equations (3) and (4) are strictly valid only for very small Reynolds numbers, N_{Re}. That is,

$$N_{Re} = \frac{d_p u_r \rho_G}{\mu_G} \rightarrow 0 \tag{5}$$

where "ρ_G" is the gas density. According to Schlichting (1968), equation (3) may be considered satisfactory for:

$$N_{Re} < \sim 1 \tag{6}$$

For larger Reynolds numbers, equation (4) can be written in the form:

$$F_r = - C_D \left(\frac{\pi \, d_p^2 \, \rho_G \, u_r^2}{8C'} \right) \tag{7}$$

where "C_D" is the drag coefficient. The drag coefficient for various Reynolds number ranges can be obtained from equations (8), (9), and (10), as presented by Fuchs (1964).

$$\text{Stokes' Law} \quad \left(N_{Re} < \sim 1\right) \quad C_D = \frac{24}{N_{Re}} \tag{8}$$

$$\text{Oseen's solution} \quad \left(N_{Re} < \sim 3\right) \quad C_D = \frac{24}{N_{Re}} \left(1 + \frac{3}{16} N_{Re}\right) \tag{9}$$

$$\text{Klyachko's solution} \quad \left(3 < N_{Re} < 400\right) \quad C_D = \frac{24}{N_{Re}} + \frac{4}{\left(N_{Re}\right)^{1/2}} \tag{10}$$

Drag coefficients also are presented by Lapple and Shepherd (1940) for Reynolds numbers from 0.1 to over 1,000,000.

The Reynolds number is a function of temperature and pressure through the kinematic viscosity, ν_G, defined as:

$$\nu_G = \frac{\mu_G}{\rho_G} \tag{11}$$

At a given pressure, high temperatures cause large kinematic viscosities and thus result in relatively small Reynolds numbers. At a given temperature, high pressure reduces the kinematic viscosity and thus results in a larger Reynolds number. At higher pressure the gas is more dense and therefore the inertia of the displaced gas becomes more important. At high temperatures, the gas is both less dense and more viscous so that the inertia of the displaced gas is much less important in comparison to the viscous forces. Figure 2 shows the kinematic viscosity of air as a function of temperature and pressure.

The Reynolds number [equation (5)] also depends on the particle velocity relative to the gas. For a given particle velocity and diameter, Figure 3 may be used to determine the region in which the drag coefficient is given by Stokes' Law [equation (8)]. For example, if the particle velocity is 100 cm/s, the vertical axis reads directly as particle diameter in microns. The area below each curve is the region in which equation (8) is adequate. Therefore the drag coefficient for a 5 μm diameter particle moving at 100 cm/s would be given by equation (8) for all temperatures shown at atmospheric pressure. At a pressure of 15 atm, equation (8) would only apply for temperatures larger than about 890°C. Figure 4 is an expansion of the vertical axis in Figure 3. Where equation (8) is not sufficiently accurate, equations (9) or (10), or the drag coefficients presented by Lapple and Shepherd (1940) should be used.

If it is assumed that equation (4) is valid at high temperature and pressure, the effects of temperature and pressure will be contained in the terms "μ_G" and "C'". For most collection mechanisms, the particle deposition velocity is inversely proportional to the gas resistance force, and therefore proportional to the ratio "C'/μ_G". The effects of high temperature and pressure on the ratio "C'/μ_G" for air, are plotted as a function of particle diameter in Figure 5. "C'" was calculated from equation (12) presented below.

At atmospheric pressure (solid lines), and for particles larger than a few tenths of a micron in diameter, the ratio "C'/μ_G" decreases with increasing temperature. This is because the gas is more viscous at higher temperature and therefore is more resistant to particle motion relative to the gas stream. For large particles, "C'" becomes very nearly unity and the

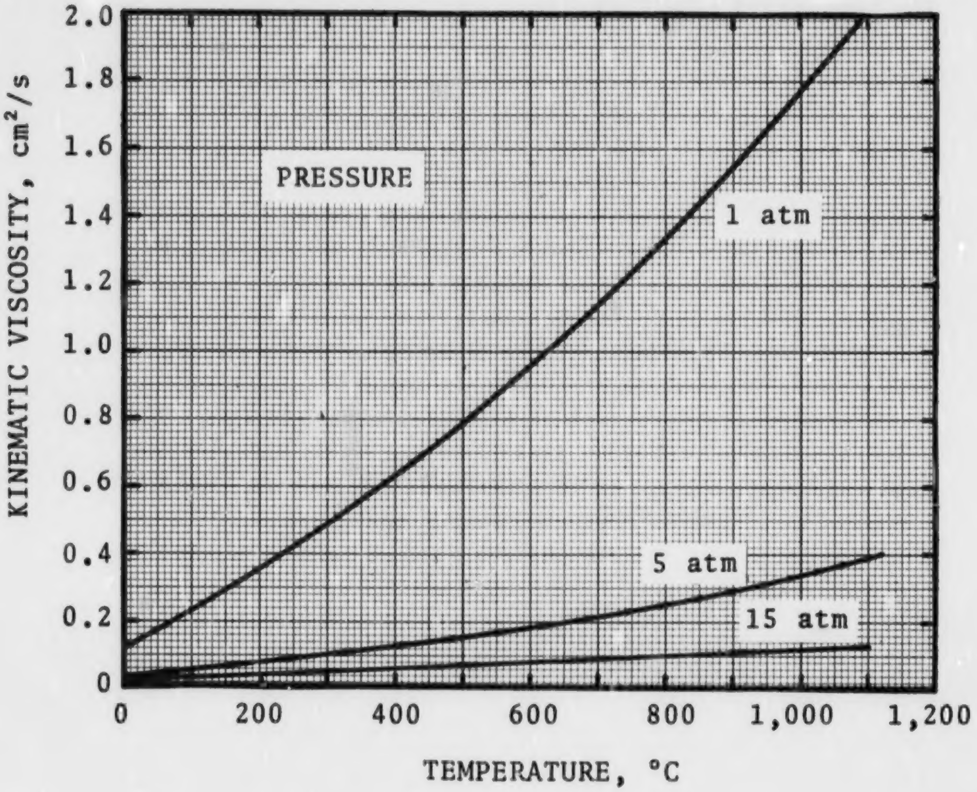

Figure 2. The effect of temperature and pressure on the kinematic viscosity of air.

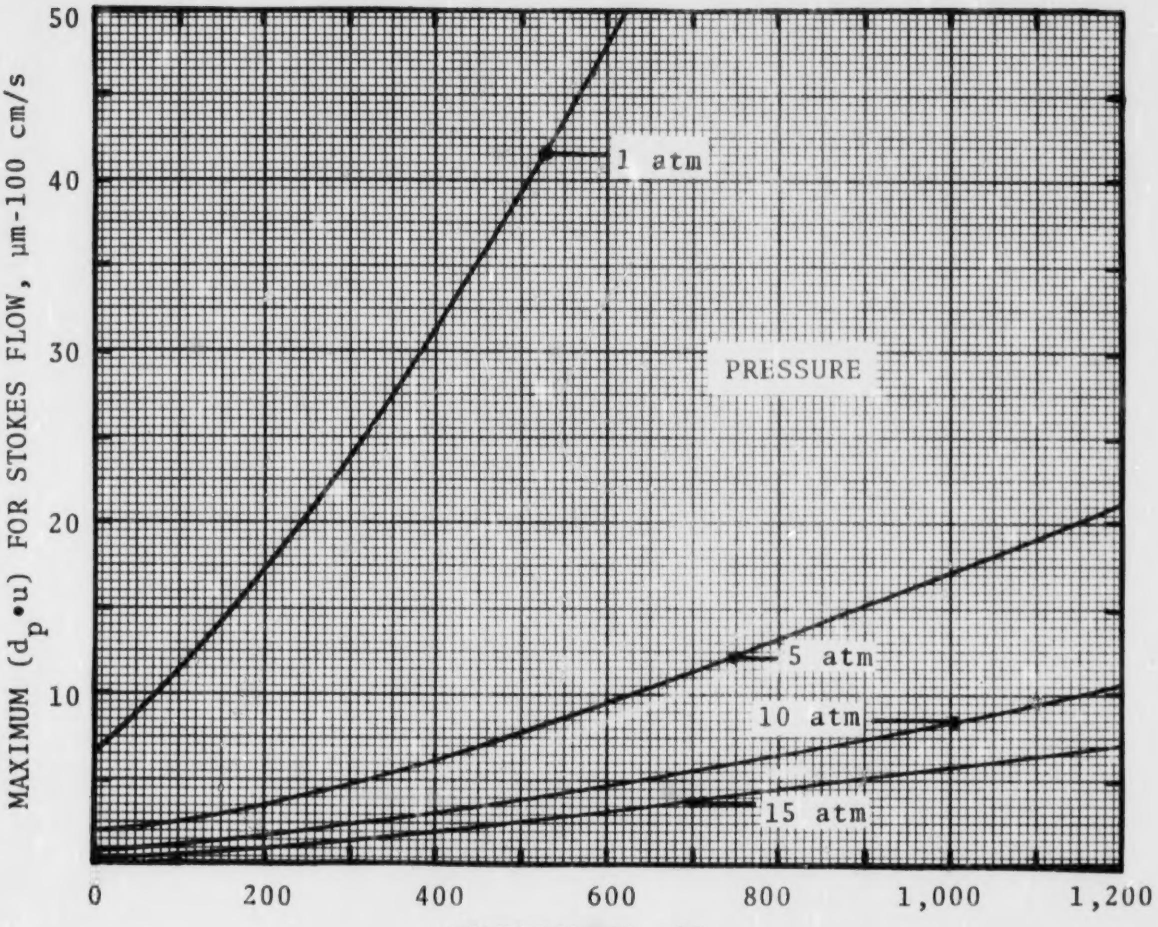

Figure 3. Validity of Stokes' law at high temperature and pressure.

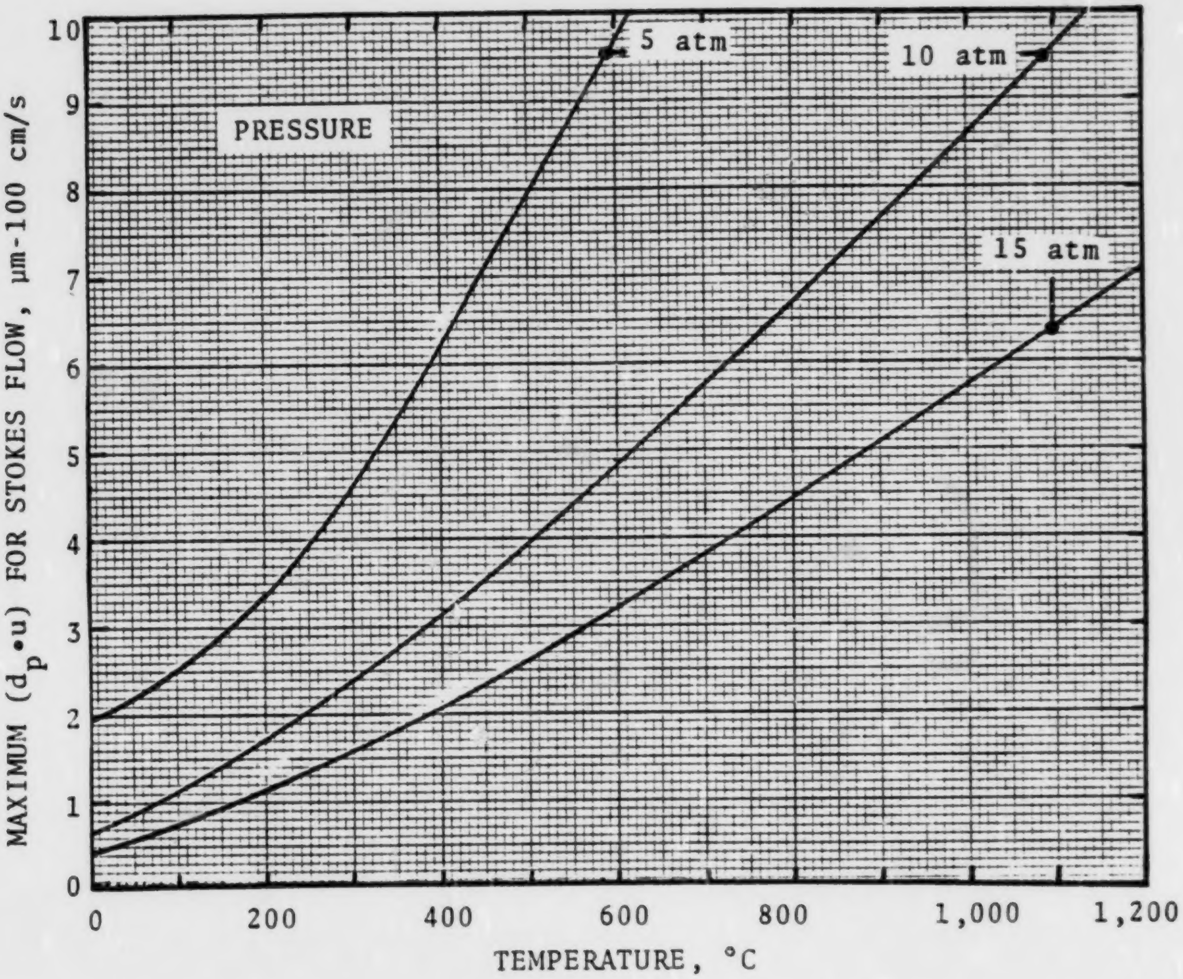

Figure 4. Validity of Stokes' law at high temperature and pressure.

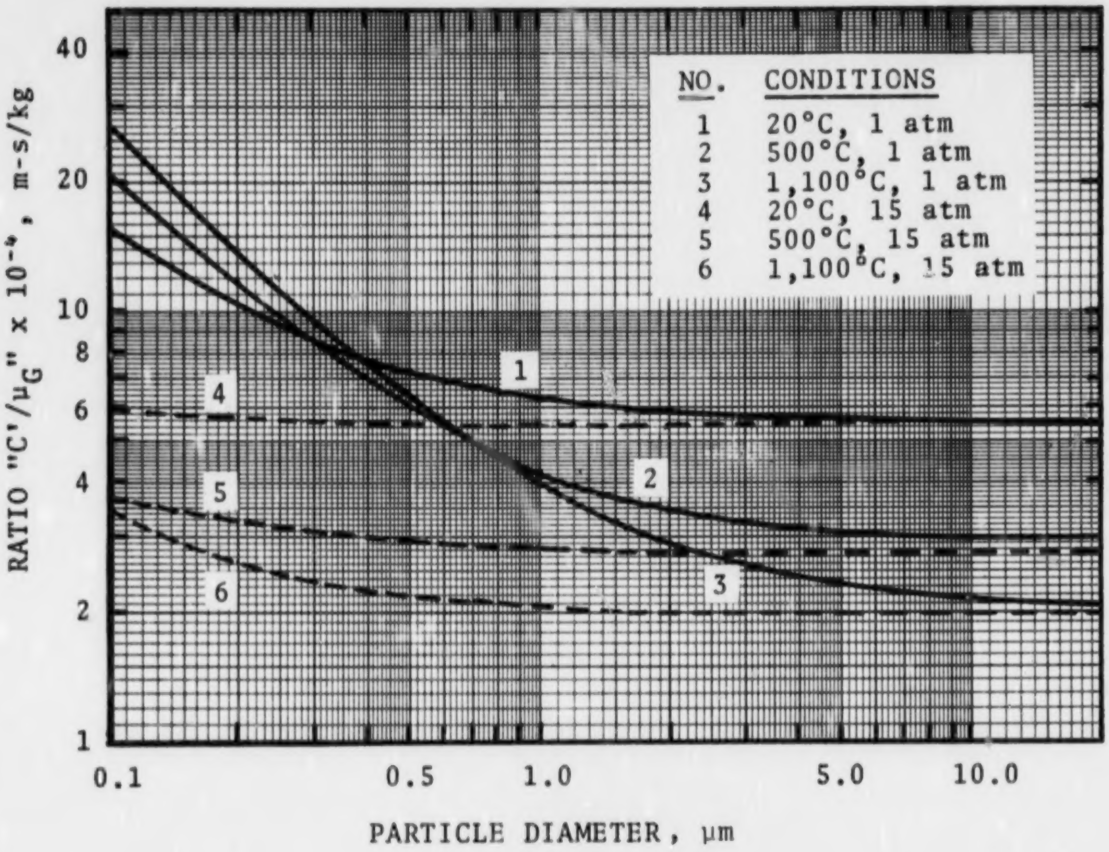

Figure 5. The effect of temperature and pressure on the ratio of the Cunningham slip correction factor to the dynamic viscosity of air.

ratio "C'/μ_G" becomes independent of particle size. The fluid resistance force is still a function of particle diameter [equation (4)] but the temperature and pressure functionality of the resistance force becomes independent of particle size. For small particles, the ratio "C'/μ_G" increases with increasing temperature because the larger molecular mean free path at high temperature causes a decrease in the gas resistance and hence an increase in "C'".

At 15 atm pressure, the molecular mean free path is reduced and "C'" is near unity, even for small particles and high temperatures. The effect of high pressure, therefore, is to increase the resistance force on very small particles, and hence decrease the ratio "C'/μ_G".

SLIP CORRECTION FACTOR

The major uncertainty in the use of equation (4) at high temperatures and pressures is in the Cunningham slip correction factor, C', used to modify Stokes' Law. It is an empirical factor generally based on the data of Millikan (1923a, b), and is given by Davies (1945) as:

$$C' = 1 + N_{Kn} \left| 1.257 + 0.400 \exp\left(-1.10/N_{Kn}\right) \right| \qquad (12)$$

where "N_{Kn}" is the Knudsen number, defined by:

$$N_{Kn} = \frac{2\lambda}{d_p} \qquad (13)$$

and where "λ" is the mean free path of the gas molecules. The temperature and pressure dependence of the mean free path is discussed later, in the section concerned with gas properties.

The constants in equation (12) are based on experimental data for Knudsen numbers from 0 to greater than 100 (Millikan, 1923b). The experiments were at low pressure (about 0.003 atm) and room temperature (20°C to 25°C). Therefore some consideration must be given to their applicability at high temperatures and pressures.

Equation (12) may be written in the general form:

$$C' = 1 + N_{Kn}\left[A + B\exp\left(-c/N_{Kn}\right)\right] \tag{14}$$

Equation (14) may then be broken down into the two cases:

$$C' = 1 + A\,N_{Kn} \tag{15}$$

for small N_{Kn}; and

$$C' = 1 + (A + B)N_{Kn} \tag{16}$$

for large N_{Kn}. The constant "c" in equation (14) is used to bridge equations (15) and (16) for intermediate Knudsen numbers.

The theoretical basis for equation (15) was discussed by Millikan (1923a), and for air and oil drops at 23°C:

$$A = 0.998\left(\frac{2}{\alpha_m} - 1\right) \tag{17}$$

where "α_m" is the fraction of molecules that are diffusely reflected from the particle surface. The constant "0.998" was obtained using the definition of the mean free path presented by Davies (1945) and attributed to Chapman and Enskog [see equation (55)]. Millikan states that equation (17) is valid as long as the term "$2/\alpha_m$" is not very large compared to unity.

At large Knudsen numbers, the gas molecules are independent of each other and the particle is in the free molecular regime. The drag force on the particle depends on the momentum transfer between the gas molecules and the particle surface. Millikan (1923b) showed that equation (16) is also a function of "α_m" and determined bounds for the constant "A+B". That is,

$$(A + B) = 2.455 \qquad \text{for } \alpha_m = 0 \tag{18}$$

$$(A + B) = 1.612 \qquad \text{for } \alpha_m = 1 \tag{19}$$

Therefore, the constants in equation (14) are a function of the momentum transfer between the gas molecules and the particle surface, and most likely are bounded by equations (17), (18) and (19). The effects of temperature and pressure on the constants in equation (14) will come in through the factor "α_m", which may be considered as a momentum accommodation coefficient.

A recent paper by Willeke (1976) discusses the temperature dependence of particle slip in a gaseous medium. He considered temperatures up to 727°C (1,000°K). He assumed that Millikan (1923a) had recorded the maximum range of reflection coefficients (momentum accommodation), and estimated that the maximum error in the drag force (and hence slip correction) resulting from a lack of knowledge of the exact degree of accommodation would be ±3%.

The maximum range of reflection coefficients found by Millikan was from 0.79 (air-fresh shellac) to 1.00 (air-mercury). These measurements were at room temperature. It is possible that at extreme temperatures, the degree of accommodation could be even lower than that measured by Millikan.

Wachman (1962) reviewed the theory and experimental data for momentum transfer between free molecules and surfaces. He showed that the drag coefficient is proportional to the square root of the energy (thermal) accommodation coefficient, α_t, where "α_t" generally can be expressed by:

$$\alpha_t = \frac{T_r - T_g}{T_s - T_g} \tag{20}$$

and where "T_g" is the absolute temperature of the incident gas molecule, "T_r" is the temperature of the reflected gas molecule, and "T_s" is the temperature at the particle surface.

The experimental data reviewed by Wachman (1962) generally showed "α_t" decreasing with increasing gas temperature. This would imply that the drag coefficient, and hence "α_m" would also decrease with increasing temperature and thereby influence the constants in equation (14). The accommodation coefficient was found to be independent of gas pressure.

Other authors have also found the accommodation coefficients to decrease with increasing temperature, including: Stickney (1962), Wachman (1966), Goodman and Wachman (1967), Byers and Calvert (1967), Goodman (1969), and Ramesh and Marsden (1974).

Ramesh and Marsden (1974) obtained the following empirical equation for the slope of the "α_t" versus surface temperature curve, for nitrogen impinging on a surface.

$$\frac{d\ \alpha_t}{d\ T_s} = (-13.7 + 0.09\ M_s) \times 10^{-4} \qquad (21)$$

where "M_s" is the molecular weight of the surface material. From equation (21), it can be predicted that "α_t" will decrease with increasing temperature for any surface material whose molecular weight is less than about 150. If it is assumed that fly ash is 50% SiO_2, 25% Fe_2O_3, and 25% Al_2O_3, then the average molecular weight will be approximately 100.

From the above discussion, it can be inferred that high temperature drag forces will be smaller than would be predicted by using equations (4) and (12). The constants in equation (12) should increase with temperature to account for the less efficient momentum transfer between the molecules and the surface observed at high temperatures. These observations, however, were based on data taken with clean, pure surfaces, and gases. Wachman (1962) notes that the accommodation coefficient can increase significantly with the buildup of an adsorbed gas layer on the surface. Therefore it is not possible to infer any quantitative information concerning the accommodation coefficient of effluent gases on fly ash particle surfaces.

If the constants in equation (14) are bounded by equations (18) and (19), the maximum increase in "C'" for large Knudsen numbers would be about 1½ times (that is, if α_m decreases from 1 to 0). For small Knudsen numbers, the increase in "C'" would probably be smaller (because N_{Kn} is smaller) but equation (17) is not valid as $\alpha_m \rightarrow 0$, so the maximum allowable size of the constant "A" in equation (14) cannot be determined.

In conclusion, therefore, it will be necessary to conduct an experimental study to determine the value of "C'" at high temperature. From the above discussion it is expected that at high temperature, "C'" will be larger than predicted by equation (12).

COLLECTION MECHANISMS

In this section, the effects of temperature and pressure on particle collection mechanisms and particle agglomeration mechanisms are reviewed. In all cases, the resistance of the gas has been assumed to be as predicted by equation (4). The validity of equation (4) at high temperatures and pressures is the major uncertainty in the theory presented below.

INERTIAL IMPACTION

One of the most important mechanisms for the collection of particles greater than a few tenths of a micron in diameter is inertial impaction. Inertial impaction is the collection of moving particles by impinging them on some target. The relative effect of inertial impaction for different particles and flow conditions may be characterized by the inertial impaction parameter, "K_p", defined as:

$$K_p = \frac{C' \rho_p d_p^2 u_G}{9 \mu_G d_c} \tag{22}$$

where "ρ_p" is the particle density, "u_G" is the gas velocity, and "$d_c/2$" is a characteristic length for the collector.

The inertial impaction parameter is equivalent to the ratio of the particle stopping distance, "x_s", to "$d_c/2$". The particle stopping distance is that distance the particle would travel before coming to rest if injected into a still gas at a velocity "u_G", when only the fluid resistance force acts on the particle. By considering the particle stopping distance divided by "u_G", the particle's inertia can be characterized by a relaxation time, "τ", defined as:

$$\tau = \frac{x_s}{u_G} = \frac{K_p d_c}{2 u_G} = \frac{C' \rho_p d_p^2}{18 \mu_G} \tag{23}$$

A large relaxation time indicates that a particle will take a relatively longer time to come to equilibrium with the gas stream when injected into the stream with some initial velocity. Therefore a larger relaxation time implies that the particle encounters less viscous resistance relative to its momentum in the gas stream. Figures 6a and 6b show the effect of high temperature and pressure on the particle relaxation time, plotted as a function of the actual particle diameter (for unit density particles).

In Figure 6a, curve 1 is for standard conditions while curves 2 and 3 are for elevated temperatures and pressures. The curvature in curve 2 reflects the effect of high temperature on the molecular mean free path, and thus on the viscous drag of the gas on small particles. Curve 3 shows that high pressure effectively nullifies any beneficial effects of high temperature at small particle diameters.

Below a few tenths of a micron, inertial forces are so small that impaction is not an effective collection mechanism. Therefore the reduced drag noticed at high temperatures for very small particles may not have much significance.

Figure 6b shows the effect of high pressure at low temperature. It is apparent that high pressure particle collection by inertial forces will be somewhat more difficult than low pressure collection. However, this effect is only significant for submicron particles.

The inertial impaction parameter [equation (22)] is obtained by non-dimensionalizing the particle's equations of motion. The equations of motion are derived from Newton's second law of motion and the modified Stokes' law [equation (4)], assuming only the drag force acts on the particle. The characterization of inertial impaction by the impaction parameter of equation (22) should be as valid at high temperature and pressure as the assumption of the modified Stokes' law.

DIRECT INTERCEPTION

A particle is collected by interception when its surface (not center of mass) touches the surface of the collector. This

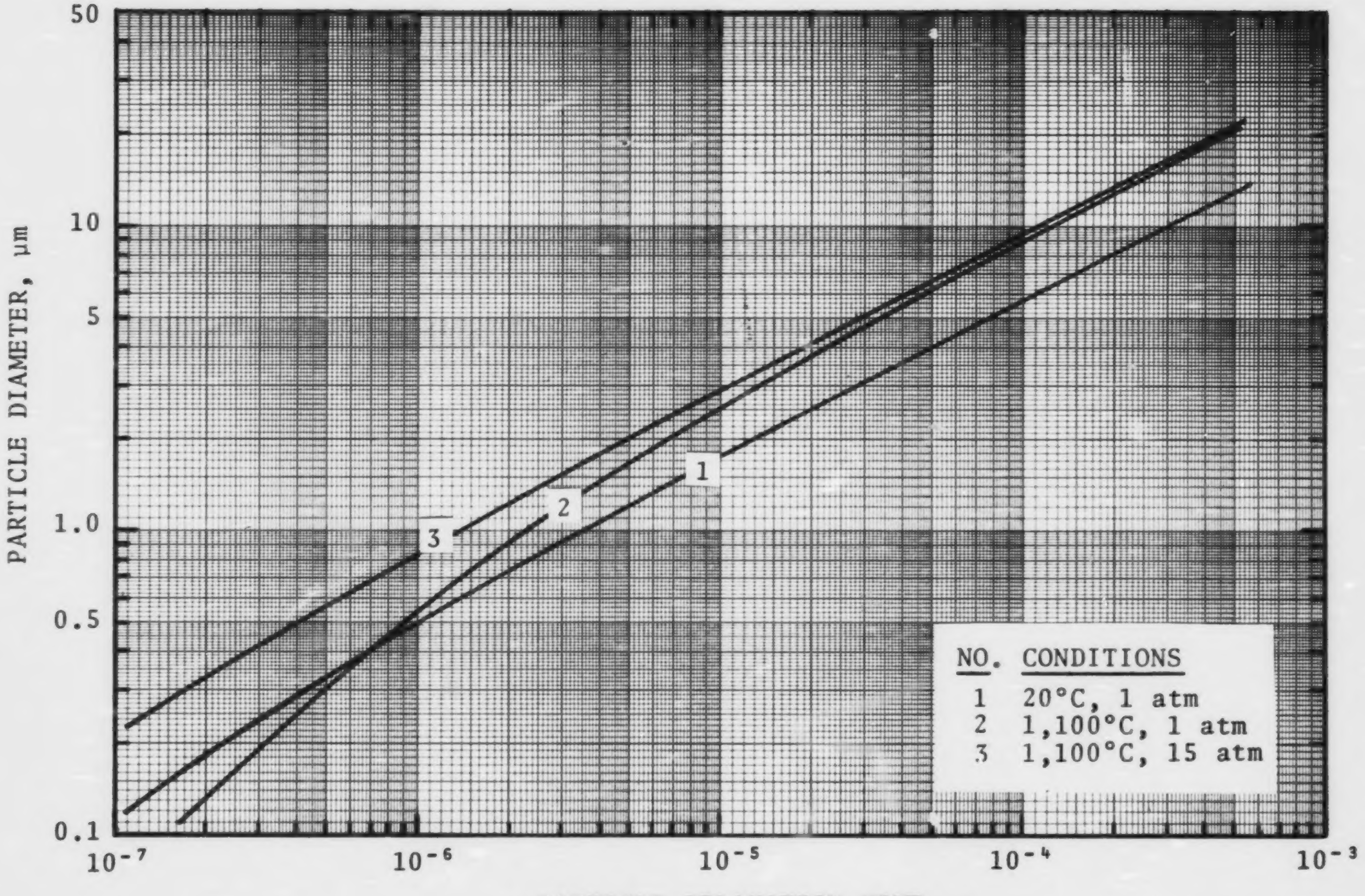

Figure 6a. The effects of temperature and pressure on the particle inertial relaxation time.

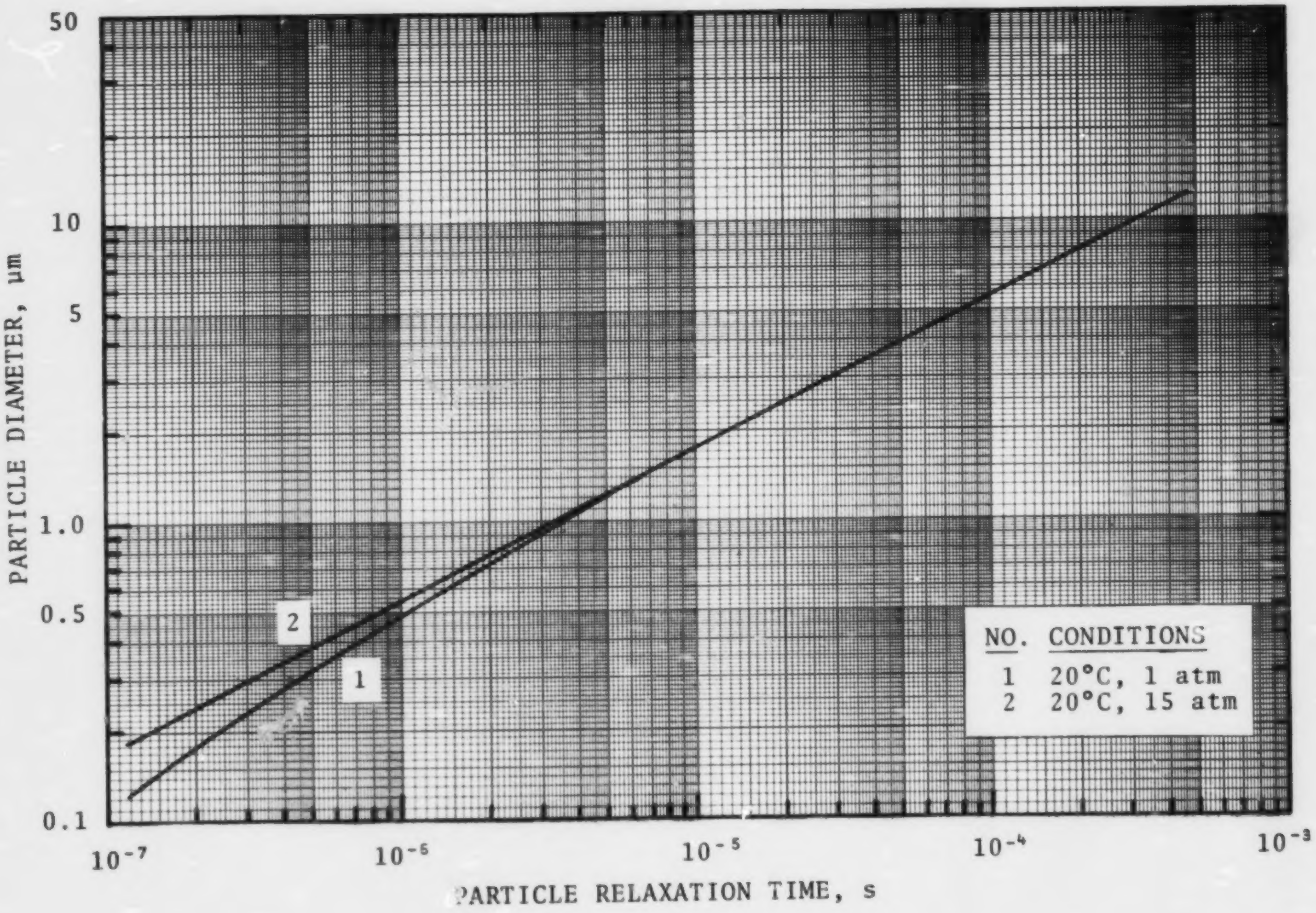

Figure 6b. The effects of temperature and pressure on the particle inertial relaxation time.

can happen without crossing any gas streamlines. Thus interception occurs if the streamline the particle rides on passes within one particle radius from the collector surface.

Interception is a function of the relative dimensions of the particle and the collector, and of the flow field. The flow field, or pattern of streamlines, is a function of the characteristic Reynolds number. The effect of increased temperature and pressure will be on the kinematic viscosity and therefore on the Reynolds number. The kinematic viscosity of air was presented as a function of temperature in Figure 2.

For a circular cylinder, Fuchs (1964) predicts the increase in impaction efficiency resulting from interception, $\Delta\eta_i$, will be a function of the Reynolds number as follows:

$$\Delta\eta_i \propto \frac{1}{(2 - \ell n\ 2N_{Ref})} \tag{24}$$

where "N_{Ref}" is the Reynolds number based on the cylinder diameter and free stream velocity. Equation (24) is valid only for small Reynolds numbers ($N_{Ref}<1$). The term "$(2 - \ell n\ 2N_{Ref})^{-1}$" is plotted as a function of "N_{Ref}" in Figure 7. It can be seen that "$\Delta\eta_i$" will increase very slowly as the Reynolds number increases from near zero towards one. This is consistent with the explanation that the collection efficiency decreases with decreasing Reynolds number because of the increased boundary layer thickness (and hence greater displacement of the streamlines from the surface) which occurs at low Reynolds numbers.

The effect of high temperature will be to increase the kinematic viscosity and therefore decrease the Reynolds number for the same free stream velocity. This will cause a larger boundary layer and hence less interception.

The effect of high pressure will be to increase the gas density and thereby increase the Reynolds number. The boundary layer thickness will thus be smaller and there will be more interception. Equation (24) is not valid at large Reynolds numbers, but the qualitative relationship between Reynolds number

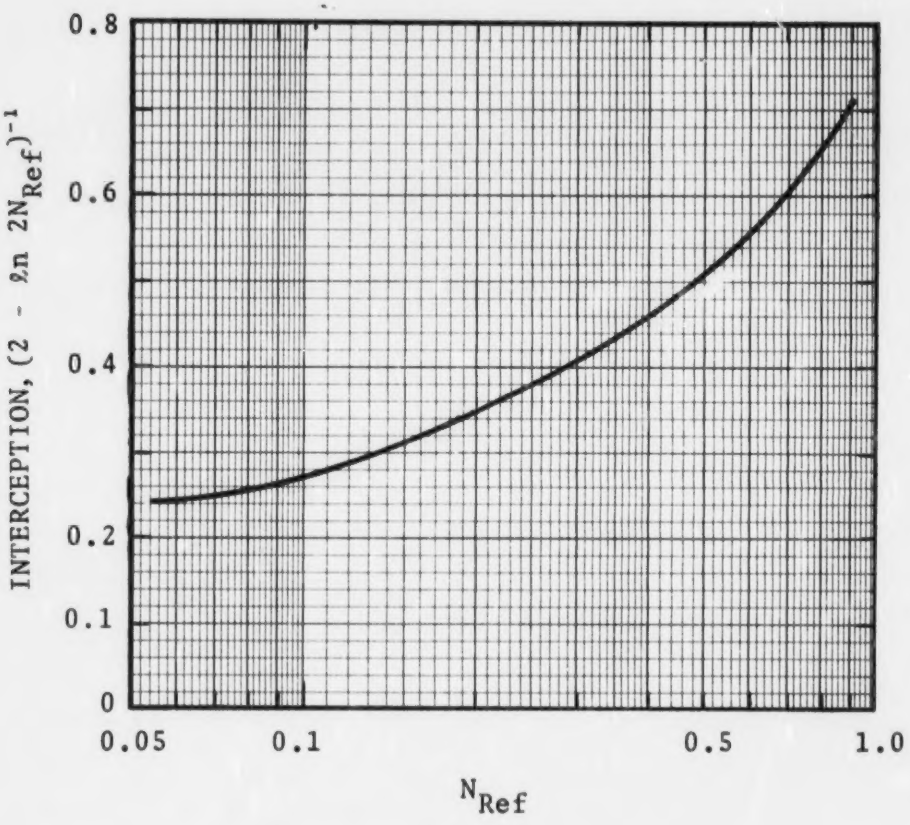

Figure 7. The effect of interception on the particle collection efficiency by a circular cylinder.

and the boundary layer thickness will be valid. That is, from Schlichting (1968):

$$\delta \propto (N_{Ref})^{-\frac{1}{2}} \tag{25}$$

where "δ" is the boundary layer thickness.

BROWNIAN DIFFUSION

Small particles can undergo significant Brownian motion resulting from the random bombardment of the particles by gas molecules. The rate of diffusion is characterized by the particle diffusivity, D_p, which may be determined from the Stokes-Einstein equation:

$$D_p = \frac{C' \; k \; T}{3\pi \; \mu_G \; d_p} \tag{26}$$

where "k" is Boltzmann's constant, and "T" is absolute temperature.

Particle diffusivities in air are shown in Figure 8 for various temperature and pressure conditions. Curve 1 is for standard conditions, while curves 2, 3, and 4 are for elevated temperature and/or pressure conditions. Particle diffusivity increases with increasing temperature, but decreases with increasing pressure.

It is often assumed that Brownian diffusion is not a significant collection mechanism for particles larger than about 0.5 μm. If this is true at standard conditions, Figure 8 indicates that diffusion would become important for particles smaller than 0.8 μm at 1,100°C and 15 atm, and for particles smaller than 1.2 μm at 1,100°C and 1 atm. Therefore the combined effect of high temperature and pressure will be to increase the particle diffusivity and thus to increase the particle size for which diffusion is significant.

Equation (26) is based on the equation derived by Einstein and presented by Fuchs (1964):

$$D_p = k \; T \; B_p \tag{27}$$

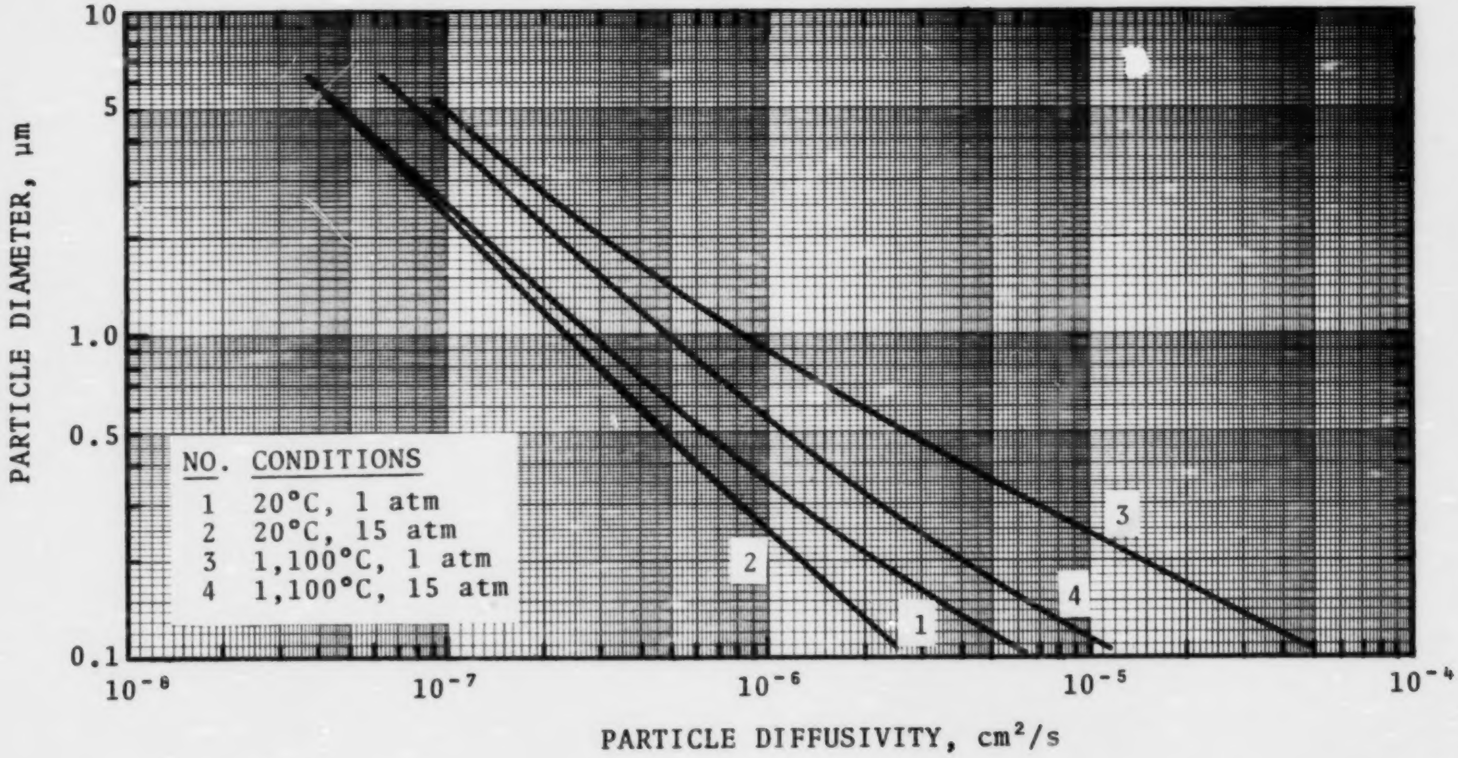

Figure 8. The effects of temperature and pressure on particle diffusivity.

where "B_p" is the particle mobility. This equation assumes that the drag force on a particle is proportional to the velocity of the particle. This assumption is valid for very small Reynolds numbers where the inertia of the fluid displaced by the particle is negligible ($N_{Re} < \sim 1$). Fuchs (1964) presents mean velocities for particles undergoing Brownian motion at standard conditions. The maximum Reynolds number occurs for the smallest particle (d_p=0.002 μm) which moves at the largest velocity (4,965 cm/s). Reynolds numbers at other temperatures and pressures can be obtained using the kinematic viscosity curves presented in Figure 2, and noting that:

$$\bar{u}_{BD} \propto (T)^{\frac{1}{2}} \qquad (28)$$

where "$\bar{u}_{BD}$" is the average velocity resulting from Brownian motion.

Particle diffusion Reynolds numbers for a variety of temperatures and pressures and for d_p=0.002 μm, are given in Table 1.

Table 1. BROWNIAN DIFFUSION REYNOLDS NUMBERS FOR A 0.002 μm DIAMETER PARTICLE AT VARIOUS TEMPERATURES AND PRESSURES

Conditions	N_{Re}
20°C, 1 atm	0.007
20°C, 15 atm	0.110
1,100°C, 1 atm	0.001
1,100°C, 15 atm	0.016

Even in the worst case (20°C, 15 atm), the Reynolds number is very small ($N_{Re} \approx 0.1$) and therefore the application of equation (27) should be valid at high temperature and pressure.

The particle mobility, B_p, is the proportionality constant between the drag force and the particle velocity, and is usually given as:

$$B_p = \frac{C'}{3\pi \mu_G d_p} \tag{29}$$

Equation (29) comes directly from the modified Stokes law. Therefore the use of equation (29) [and therefore equation (26)] at high temperature and pressure depends on the applicability of Stokes' law as discussed in the previous section.

Whenever a particle travels in a moving gas stream, it becomes necessary to consider the particle transport by convection as well as by Brownian diffusion. The Péclét number, N_{Pe}, characterizes convective transport relative to Brownian diffusion. That is:

$$N_{Pe} = \frac{\mu_G d_c}{D_p} \tag{30}$$

In general, the collection efficiency by diffusion is inversely proportional to some power of the Péclét number. The principal temperature dependent term in equation (30) is the particle diffusivity. However, the gas velocity will be a function of temperature and pressure if the mass flow rate is held constant.

Kornberg (1973) experimentally investigated the high temperature (to about 450°C) filtration of particles by diffusion, and compared his results with the theory of diffusional deposition onto single, cylindrical fibers. He assumed the Cunningham correction factor to be a function of temperature through the mean free path only. If the effects of temperature on accommodation coefficient (discussed in the previous section of this report) are important, it would be expected that the theory used by Kornberg would underestimate the experimental efficiencies. This did not appear to be the case, however the experimental uncertainty was large enough to have masked this effect.

Kornberg's results indicated that the single fiber collection efficiency by diffusion, η_s, is proportional to absolute temperature as follows:

$\eta_s \propto T^{0.815 \pm 0.300}$ experimentally, and

$\eta_s \propto T^{1.0}$ theoretically. He concluded that current diffusional filtration theory is adequate for predicting filter efficiencies at high temperatures. However, noting the experimental uncertainty, it is possible that the experimental and theoretical values of "η_s" may differ more substantially at very high temperatures (greater than ~500°C).

ELECTRICAL MIGRATION

Theoretically, the migration velocity of a particle in an electrostatic precipitator is a function of the charging and precipitating electric fields, the particle size and dielectric characteristics, and the gas viscosity and mean free path (see White, 1963). That is:

$$u_e = \frac{\varepsilon}{\varepsilon+2} \; \frac{C' \, \varepsilon_o \, E_c \, E_p \, d_p}{4 \, \pi \, \mu_G} \qquad (31)$$

where "u_e" is the electrical migration velocity (deposition velocity), "ε" is the particle dielectric constant, "E_c" and "E_p" are the charging and precipitating electric field strengths respectively, and "ε_o" is the permittivity constant (8.854×10^{-12} coulomb^2/nt-m^2). Equation (31) assumes that the particle is fully charged by field charging, and that the gas resistance force is given by the modified Stokes' law (equation 4).

The presence of a dielectric (resistive) particle causes a decrease in the effective voltage because of the internal voltage drop which is induced in the particle and opposite to the applied voltage. Therefore the actual voltage, E_p, is always somewhat less than the applied voltage, E_o. The dielectric constant is defined as:

$$\varepsilon = \frac{E_o}{E_p} \qquad (32)$$

Strauss (1966), states that the dielectric constant is not a significant function of temperature. Tassicker (1971) and Masek (1973), however, have measured dielectric constants for fly ash in AC electric fields and found that they are a function of temperature at least up to 220°C. At low frequencies, the dielectric constant increases with increasing temperature. At high frequencies it is relatively independent of temperature.

The possible increase in the dielectric constant at high temperature would not change the migration velocity very much. At very large values of the dielectric constant, the term "$\varepsilon/(\varepsilon+2)$" approaches unity. At normal temperature values of the dielectric constant (for fly ash, $\varepsilon \approx 3$):

$$\frac{\varepsilon}{\varepsilon+2} \approx 0.6 \qquad (33)$$

Therefore the maximum possible increase in the migration velocity resulting from an increase in the dielectric constant would be about 1.7 times.

Equation (31) is based on the assumption that the particle is fully charged by field charging. A larger dielectric constant means that the particle can maintain a larger maximum charge. If "ε" increases with temperature, therefore, the total charge that a particle can hold will increase.

Equation (31) is also based on the assumption of Stokes' law for the gas resistance force. Thus the temperature and pressure dependence comes in through the ratio "C'/μ_G". White (1963) calculated migration velocities for temperatures of 20°C and 350°C, and predicted that they would decrease by a factor of about 0.6 at the higher temperature. These predictions were not verified theoretically.

High temperature and pressure also affect the formation and operation of DC corona, and the current-voltage characteristics of electrical precipitators. A detailed survey of these effects is outside the scope of the present study. In general, however, the corona starting voltage and the sparkover voltage decrease with increasing temperature. The sparkover voltage, however, decreases more rapidly so that the voltage operating range decreases with increasing temperature. Corona starting voltages and sparkover voltages increase with gas density, and therefore high pressure alleviates some of the problems associated with high temperature precipitation.

Another effect of high temperatures is on the charging of particles. Field charging is a result of the bombardment of the particles by gas ions in the ionic current, and is the primary charging mechanism for particles larger than a few tenths of a micron in diameter. The saturation charge, q_s, acquired by a particle by ionic bombardment is:

$$q_s = \frac{3\varepsilon}{\varepsilon+2} \frac{\varepsilon_o E_c d_p^2}{4} \tag{34}$$

For a given electric field, equation (34) will be a function of temperature only through the dielectric constant, ε. However, the rate of particle charging, as pointed out by Strauss (1966), is inversely proportional to the ion mobility, B_i, and therefore proportional to the absolute pressure, P, and to the inverse square root of the absolute temperature. That is:

$$B_i \propto \frac{T^{\frac{1}{2}}}{P} \tag{35}$$

For very small particles, ion diffusion becomes an important particle charging mechanism. Strauss (1966) presented a table, attributed to Lowe and Lucas, comparing the numbers of charges acquired by a particle by ion bombardment and by ion diffusion. This table is reproduced as Tables 2a and 2b.

Table 2. NUMBERS OF CHARGES ACQUIRED BY A PARTICLE
Tables 2a and 2b are from Strauss (1966).

a. Ion Bombardment

Particle Diameter, µm	Period of exposure, s 0.01	0.1	1	∞
0.2	0.7	2	2.4	2.5
2.0	72	200	244	250
20.0	7,200	20,000	24,400	25,000

b. Ion Diffusion, 27°C

Particle Diameter, µm	Period of exposure, s 0.01	0.1	1	10
0.2	3	7	11	15
2.0	70	110	150	190
20.0	1,100	1,500	1,900	2,300

c. Ion Diffusion, 1,100°C

Particle Diameter, µm	Period of exposure, s 0.01	0.1	1	10
0.2	9	25	43	62
2.0	250	440	630	820
20.0	4,400	6,300	8,200	10,100

The charge, q_p, acquired by ion diffusion may be calculated from:

$$q_p = \frac{d_p\ k\ T}{2e}\ \ell n \left[1 + \frac{\pi\ d_p\ \bar{c}\ N_i\ e^2}{2\ k\ T}\ t \right] \tag{36}$$

where "e" is the unit electronic charge ($4.8\text{x}10^{-10}$ e.s.u.), "$\bar{c}$" is the root mean square molecular velocity, "N_i" is the number of ions per unit volume, and "t" is time. The acquired charge is proportional to absolute temperature.

Using the same numbers used by Lowe and Lucas, but a temperature of 1,100°C, Table 2c was obtained for comparison to Tables 2a and 2b. It is apparent that diffusion charging should be much more important at high temperatures, and is the dominant charging mechanism for particles up to a few microns in diameter.

GRAVITATIONAL SETTLING AND CENTRIFUGAL SEPARATION

The gravitational settling velocity, u_s, and the deposition velocity of a particle in a centrifugal force field, u_c, may be approximated as:

$$u_s = \frac{1}{18}\ \frac{C'\ d_p{}^2(\rho_p - \rho_G)\ g}{\mu_G} \tag{37}$$

$$u_c = \frac{1}{18}\ \frac{C'\ d_p{}^2(\rho_p - \rho_G)\ u_t{}^2}{\mu_G\ R} \tag{38}$$

where "ρ_p" and "ρ_G" are the densities of the particle and gas, "g" is the acceleration of gravity, "u_t" is the tangential particle velocity at radius "R".

Equations (37) and (38) were derived using the modified Stokes' law for the gas resistance force. Therefore the ratio "C'/μ_G" contains the major temperature and pressure dependence. The gas density also depends on temperature and pressure, however even at high gas density (ρ_G=0.018 g/cm³ at 15 atm and 20°C) the density is less than one percent of typical particle densities (ρ_p=2 to 3 g/cm^3).

The tangential velocity in equation (38) is a function of the inlet velocity to the cyclone. Therefore, for the same mass flow rate, increases in temperature and pressure will affect the volumetric flow rate and hence the gas velocity. High pressure will decrease the gas velocity while high temperature will increase it. The application of cyclones at high temperature and pressure is discussed in a later section.

THERMOPHORESIS

Temperature gradients can give rise to deposition forces which can improve the collection efficiency of particulate control devices.

Thermophoresis is the result of gas molecules impinging on the particle surface from opposite sides with different mean velocities. The particle receives a net impulse opposite to the temperature gradient in the gas. The magnitude of the thermophoretic force was first devised by Epstein (1929), and may be used with equation (4) for the resistance force, to obtain the thermophoretic deposition velocity, u_d, as:

$$u_d = -\frac{3}{2}\frac{C'\ \mu_G}{\rho_G\ T}\left(\frac{k_G}{2k_G + k_p}\right)\nabla T \tag{39}$$

where "k_G" is the thermal conductivity of the gas, "k_p" is the thermal conductivity of the particle, and "∇T" is the temperature gradient. The derivation of equation (39) assumes the modified Stokes' law for predicting the gas resistance force. The temperature and pressure functionality is fairly complicated because all the terms in equation (39) are temperature dependent. The individual temperature and pressure dependence of the gas and particle properties is discussed in a later section.

Figure 9 shows the effects of temperature and pressure on the thermophoretic deposition velocity per unit temperature gradient, for a 5 μm diameter silica particle, as calculated from

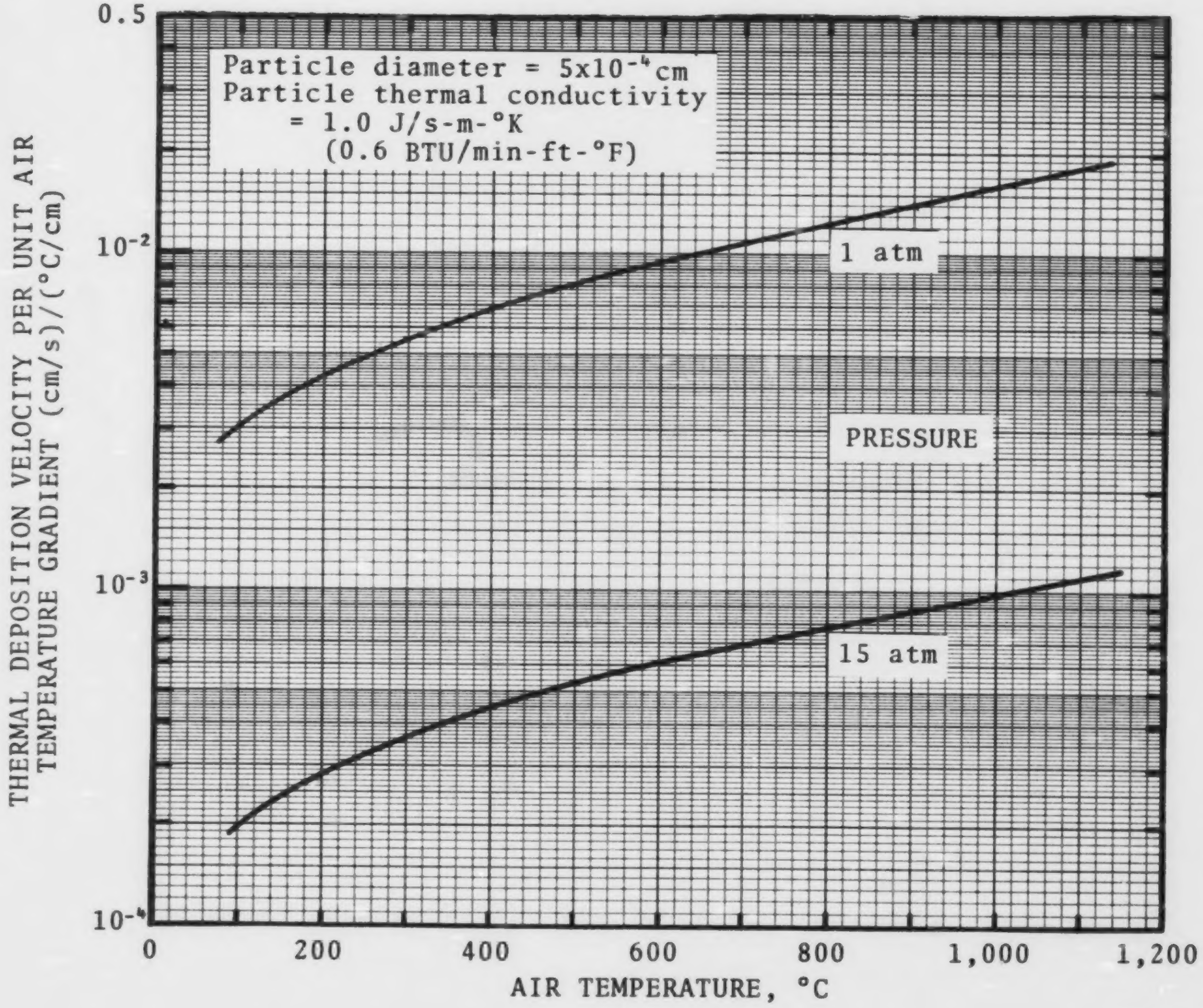

Figure 9. Thermal deposition velocity as a function of temperature and pressure.

equation (39). The deposition velocity increases slightly with increasing temperature but decreases significantly with pressure.

More elaborate equations for predicting the thermophoretic deposition velocity have been presented by Hidy and Brock (1970), and by Derjaguin and Yalamov (1972). For example, using the full set of first order slip flow boundary conditions, Brock (1962) derived the following expression:

$$u_d = -\frac{3}{2}\,\frac{C'\,\mu_G}{\rho_G\,T}\,\frac{(k_G/k_p + C_t\,N_{Kn})\,\nabla T}{(1 + 3C_m\,N_{Kn})(1 + 2k_G/k_p + 2C_t\,N_{Kn})} \qquad (40)$$

where "C_m" is the isothermal slip coefficient, and "C_t" is the temperature jump coefficient. Both "C_m" and "C_t" are functions of the energy and momentum accommodation between the molecules and the particle surface.

The temperature and pressure dependence of the accommodation coefficient was discussed in the previous section in connection with the Cunningham slip correction factor. In general, the accommodation coefficient is independent of pressure and decreases with increasing temperature (this is discussed in detail by Wachman, 1962). A decrease in accommodation coefficient means that the thermal energy and momentum exchange between the bombarding molecules and the particle is less effective. Therefore the thermal force on the particle will be weaker than it would be with perfect accommodation at a given temperature, and hence the thermal deposition velocity would be smaller.

As stated in the earlier discussion of accommodation coefficients, the gas and surface purities are very significant in predicting, quantitatively, the effects of temperature on the accommodation coefficient. Therefore, experimental measurements of the thermophoretic deposition velocity would be necessary in order to determine the significance of the temperature dependence of the accommodation coefficient.

DIFFUSIOPHORESIS

Diffusiophoresis is the transmission of particulate matter from one place to another by molecular diffusion forces. Generally, diffusiophoresis is important in situations where there are large concentration gradients, or where vapor condensation is occurring. It is unlikely that such conditions will exist in high temperature and pressure particulate removal systems. Nevertheless, diffusiophoresis may be important in situations where high pressure and low or moderate temperature particle collection is required.

Diffusiophoresis at high pressure and relatively low temperature was discussed by Calvert, et al. (1972). Following a similar theoretical approach, the diffusiophoretic deposition velocity, u_D, is given as:

$$u_D = - \frac{\sqrt{M_v}}{p_v\sqrt{M_v} + p_G\sqrt{M_G}} \; \frac{P\,D_{vG}}{p_G} \; \nabla p_v \qquad (41)$$

where "M_v" and "M_G" are the molecular weights of the vapor and gas, "p_v" and "p_G" are the partial pressures of the vapor and gas, "P" is the absolute pressure, "∇p_v" is the vapor pressure gradient, and "D_{vG}" is the intermolecular diffusivity between the vapor and gas.

The partial pressure of the vapor is a function of temperature but not of pressure. The diffusivity is also a function of temperature. The diffusivity for a water vapor - air mixture is presented later, in the section on gas properties.

Diffusiophoretic deposition velocities are illustrated as a function of vapor pressure gradient, for various temperature and pressure conditions, in Figure 10. The deposition velocity is seen to increase with increasing temperature and to decrease with increasing pressure.

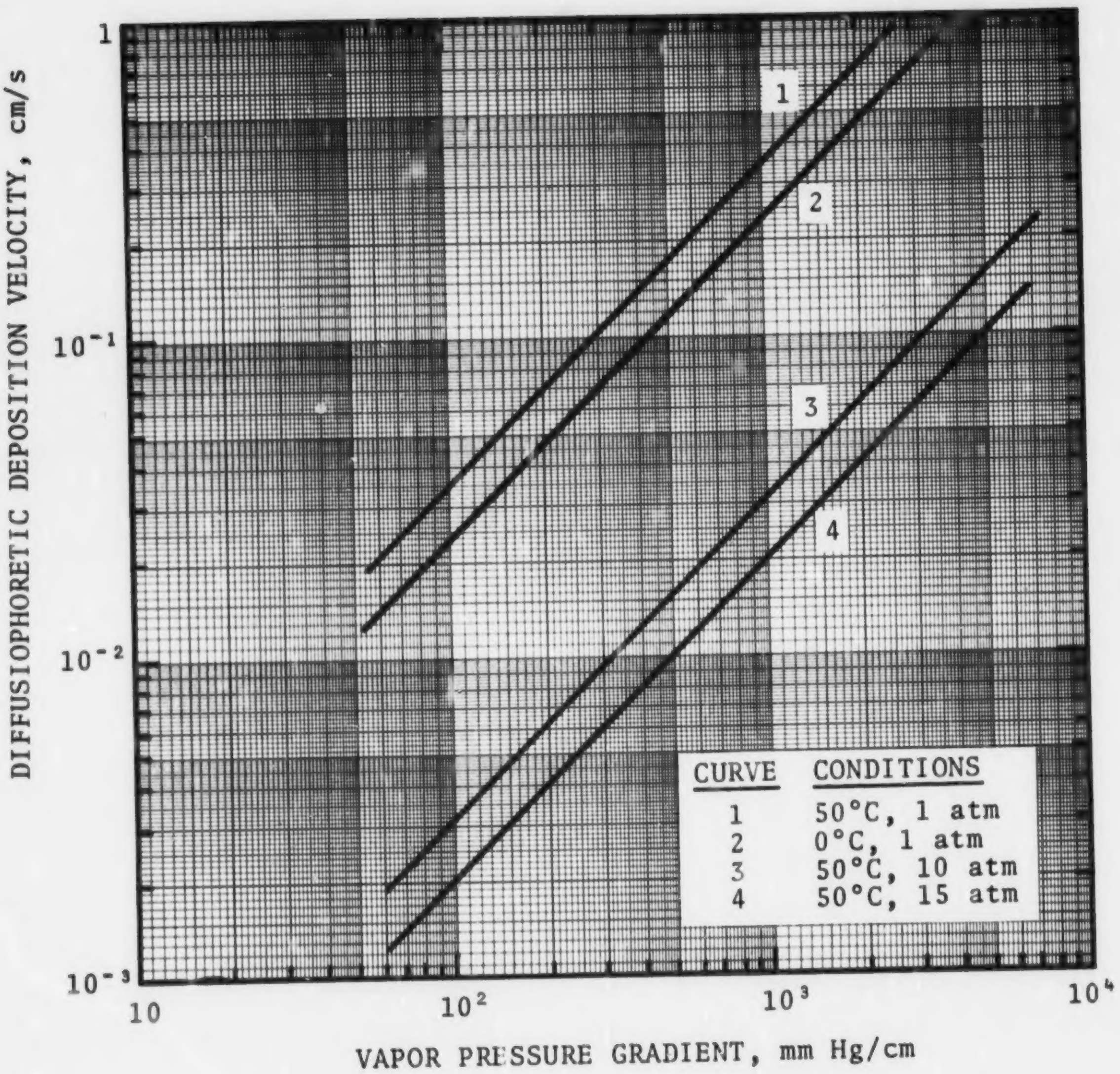

Figure 10. The effect of pressure on the diffusiophoretic deposition velocity.

PARTICLE GROWTH BY CONDENSATION

If high pressure and low temperature particle collection is required, the collection of fine particles can be improved by the condensation of vapor onto the particle, thereby increasing its size and the ease with which it can be collected by inertial methods.

After a drop of critical size has been nucleated it grows at a rate determined by the vapor pressure in the gas phase and the conditions at its surface. For a spherical, motionless drop, assuming constant drop temperature and vapor pressure, and ideal behavior of the vapors, the drop diameter can be calculated from Maxwell's equation (1890) (presented by Calvert, et al., 1972):

$$d_d^2 - d_o^2 = \frac{8}{\rho_L} \frac{D_{vG} M_v P}{R T p_{BM}} (p_\infty - p_o) t \tag{42}$$

where "d_d" is the drop diameter, "d_o" is the drop diameter at t=0, "ρ_L" is the density of the drop, "R" is the universal gas constant (8.317 J/gmole-°K), "p_∞" is the vapor pressure in the gas stream "p_o" is the vapor pressure at the drop surface, "p_{BM}" is the mean partial pressure of the non-transferring gas, and "t" is time. Equation (42) is independent of absolute pressure, and is a function of temperature directly and indirectly through the vapor pressure. The growth of particles by condensation, however, is not likely to be very important in high temperature particle removal systems.

For drops condensing while moving relative to the gas, Fuchs (1959) presents the following expression:

$$d_d^2 - d_o^2 = \frac{8}{\rho_L} \frac{D_{vG} M_v P}{R T p_{BM}} (p_\infty - p_o) t \left(1 + 0.276 N_{Re}^{1/2} N_{Sc}^{1/3}\right) \tag{43}$$

where the Reynolds number, N_{Re}, and Schmidt number, N_{Sc}, are defined as:

$$N_{Re} = \frac{\rho_G d_d u_r}{\mu_G} \tag{44}$$

$$N_{Sc} = \frac{\mu_G}{\rho_G \; D_{vG}} \tag{45}$$

and where "u_r" is the relative velocity between the drop and the gas stream.

The Reynolds number will increase with increasing pressure while the Schmidt number will decrease with increasing pressure. The term "$N_{Re}^{\frac{1}{2}} N_{Sc}^{\frac{1}{3}}$", therefore, will increase with the sixth root of pressure, or by about 50% as pressure increases from 1 atm to 15 atm. Nevertheless, the pressure dependence of equation (41) is relatively weak for normal Reynolds numbers and Schmidt numbers. The term "$x=\left(1 + 0.276\ N_{Re}^{\frac{1}{2}} N_{Sc}^{\frac{1}{3}}\right)$" is shown as a function of pressure and drop diameter in Table 3. The velocity and gas properties were assumed so that at atmospheric pressure and at d_d=1μm, $N_{Re}=N_{Sc}=1$.

Table 3. THE EFFECTS OF HIGH PRESSURE AND DROP DIAMETER ON THE GROWTH OF DROPS BY CONDENSATION

Drop Diameter	$x = 1 + 0.276\ N_{Re}^{\frac{1}{2}} N_{Sc}^{\frac{1}{3}}$	
μ_m	P = 1 atm	15 atm
1	1.00	1.43
10	1.87	2.37
100	3.76	5.33
1,000	9.73	14.71

Therefore high pressure can increase the factor "x" and thus increase the rate of particle growth by condensation.

The similar problem of liquid drop evaporation in a high temperature and high pressure environment has been investigated by Matlosz, et al. (1972). They found the effective mass diffusion coefficient to be in good agreement with theory for temperatures up to about 250°C and pressures up to about 7 atm. At a pressure of 100 atm the mass diffusion was much greater than predicted by theory.

MAGNETIC PRECIPITATION

When an electrically charged particle with no intrinsic magnetic properties moves through a magnetic field of strength, H, it will be acted on by a force at right angles to both the direction of the particle motion, and to the magnetic field lines. Therefore the particle will obtain a magnetic deposition velocity, u_m, which may be calculated from:

$$u_m = \frac{C' \mu_o H q_p u_G}{3\pi \mu_G d_p} \qquad (46)$$

where "q_p" is the particle charge, "u_G" is the gas velocity, and "μ_o" is the permeability constant ($\mu_o = 4\pi \times 10^{-7}$ V-s/A-m). Here the deposition velocity is a function of the gas velocity; the higher the gas velocity, the higher the magnetic deposition velocity.

The effects of temperature and pressure on equation (46) come in primarily through the ratio "C'/μ_G", which comes directly from the assumption of equation (4) for the gas resistance force. Also the rate at which a particle is charged is a function of temperature and pressure [equation (35)], and the amount of charge obtained by ion diffusion is a function of temperature [equation (36)].

PARTICLE AGGLOMERATION MECHANISMS

One way to improve the collection efficiency for fine particles is to cause the fine particles to agglomerate into larger aggregates which can be collected more easily.

Thermal Coagulation

Thermal coagulation is the agglomeration of particles undergoing random Brownian motion. The rate of agglomeration (or coagulation) is generally considered to be proportional to the square of the particle number concentration. That is:

$$\frac{d\ N_p}{d_t} = -K_o\ N_p^2 \tag{47}$$

where "N_p" is the particle number concentration, and "K_o" is the proportionality constant, or coagulation constant. Assuming equation (4) for the gas resistance force, Fuchs (1964) presents the following equation for the thermal coagulation coefficient of a particle undergoing Brownian motion in a still gas, assuming particles stick upon touching:

$$K_o = 4\pi\ D_p\ d_p = \frac{4}{3}\ \frac{C'\ k\ T}{\mu_G} \tag{48}$$

The thermal coagulation constant is shown as a function of temperature, pressure, and particle diameter in Figure 11. The agglomeration of particles increases with temperature and decreases with pressure. The net effect of high temperature and high pressure (20°C, 1 atm to 1,100°C, 15 atm) is to increase the rate of thermal agglomeration for a 1 μm diameter particle by a factor of 1.5 (K_o increases from 3.5×10^{-10} cm³/sec to 5.3×10^{-10} cm³/sec). For a 0.5 μm diameter particle, the agglomeration rate increases by a factor of about 1.4 (K_o increases from 3.9×10^{-10} cm³/sec to 5.6×10^{-10} cm³/sec). For a 0.1 μm diameter particle, the rate of agglomeration remains relatively constant ($K_o = 8.5 \times 10^{-10}$ cm³/sec). Therefore it appears that at high pressure and high temperature, there is a small increase in the rate of agglomeration for particles larger than 0.1 μm. At high temperature and atmospheric pressure, the rate of agglomeration of fine particles would be greatly increased; however, high pressures effectively nullify the benefit of high temperature.

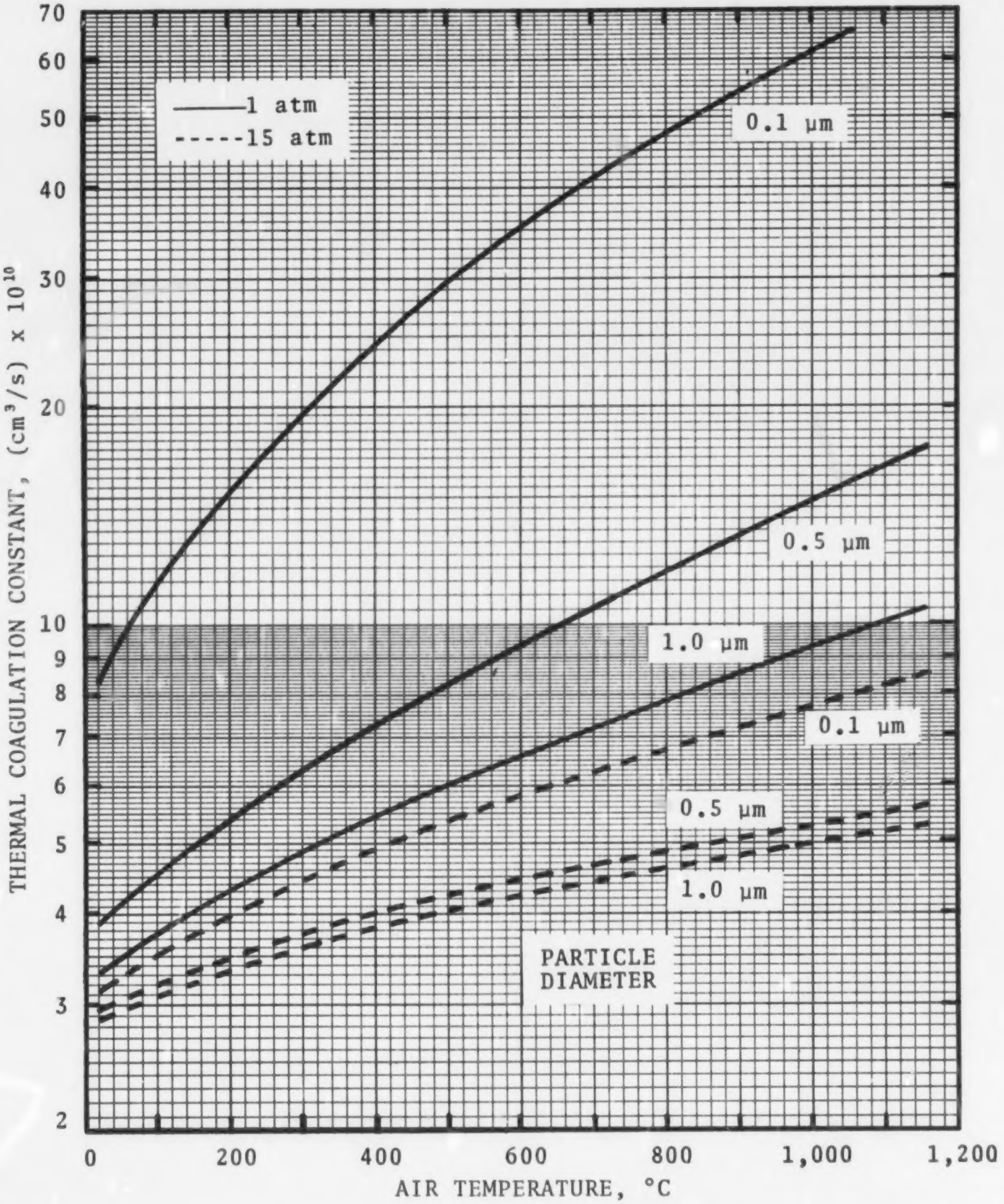

Figure 11. Thermal coagulation of particles at high temperature and pressure.

Agglomeration of Charged Particles

Thermal agglomeration can be improved if the particles are charged. Fuchs (1964) discusses this question and predicts that the coagulation constant will be increased by a factor "β" which depends on the magnitude and sign of the particle charge. That is:

$$K = \beta K_o \tag{49}$$

where "K" is the actual coagulation constant, and "K_o" is the uncharged coagulation constant of equation (48). For the case where the particles have the same charge, the rate of agglomeration decreases because of electrostatic repulsion ($\beta<1$). For particles with opposite charge, agglomeration increases because of electrostatic attraction ($\beta>1$). For a collection of charged particles with zero net charge, the arithmetic mean "β" is still slightly greater than unity. Thus even though there is no net charge, agglomeration is still greater with charged particles. Table 4 shows the effect of temperature on the thermal agglomeration of charged particles. The agglomeration of particles with like charges (β_{rep}) increases towards unity while the agglomeration of oppositely charged particles (β_{att}) decreases towards unity. The average agglomeration for a mixture of positive and negative particles with zero net charge (β_{avg}) decreases

Table 4. EFFECT OF TEMPERATURE ON THE AGGLOMERATION OF CHARGED PARTICLES

T	β_{rep}	β_{att}	β_{avg}
20°C	0.771	1.271	1.021
100°C	0.818	1.208	1.013
500°C	0.908	1.098	1.003
1,100°C	0.948	1.054	1.001

towards unity. Therefore, the net effect of temperature on the agglomeration of charged particles is to decrease the rate of agglomeration relative to uncharged particles. That is, high temperature nullifies the beneficial effect of particle charge. For a given charge on the particles, pressure should not have any effect that would not be present with uncharged particles.

Polarization Agglomeration

When a particle is under the influence of an electric field, it is inductively charged and the rate of agglomeration is affected. Fuchs (1964) discusses this problem and shows that "β" is inversely proportional to the cube root of absolute temperature. Therefore, agglomeration of inductively charged particles decreases slightly with increasing temperature.

Turbulent Agglomeration

Particles can also agglomerate as a result of turbulence in the fluid. Turbulent agglomeration has been discussed by Beal (1972) and is proportional to the turbulent diffusion coefficient. For the general case where the particle diameter is much smaller than the turbulent microscale, λ_o, Beal presents the following equation for the turbulent diffusion coefficient, D_t:

$$D_t = \frac{1}{16}\left(\frac{e_o}{\nu_G}\right)^{\frac{1}{2}} d_p^{\,2} \qquad (50)$$

where "e_o" is the energy dissipation rate for unit mass of fluid and "ν_G" is the gas kinematic viscosity. Therefore, "D_t" is proportional to "$\nu_G^{-\frac{1}{2}}$". Figure 12 is a plot of "$\nu_G^{-\frac{1}{2}}$" against temperature for a range of pressures. Turbulent agglomeration increases greatly with an increase in pressure, at low temperatures. This beneficial effect of pressure is almost completely nullified at high temperatures.

Sonic Agglomeration

Another way to cause particles to agglomerate is by the application of sonic vibrations. Sonic agglomeration has been

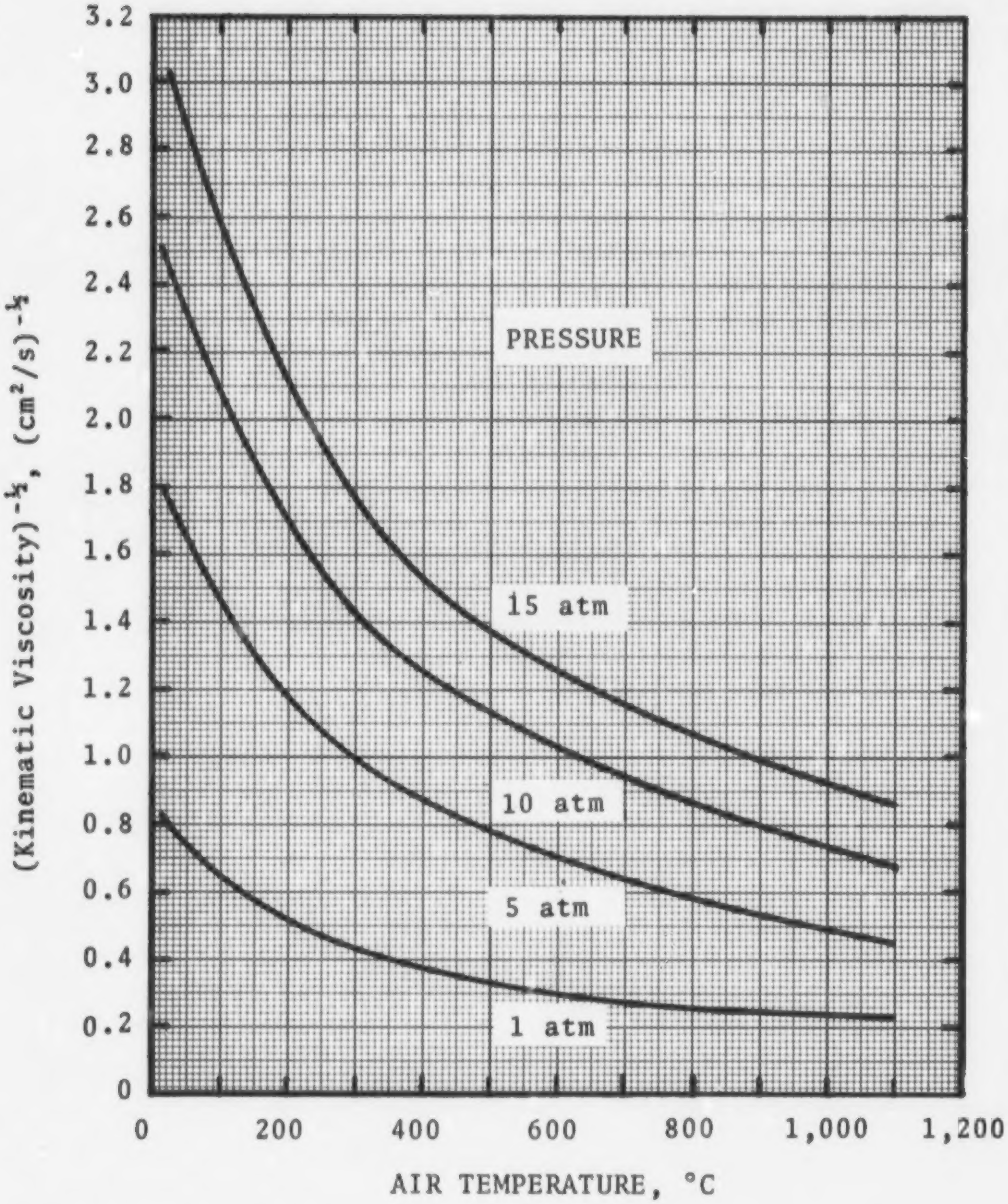

Figure 12. Turbulent agglomeration tendency of particles at high temperature and pressure.

studied by Mednikov (1965) and has been shown to be inversely proportional to the square root of the product of gas density and the speed of sound. That is:

$$K_a \propto \left(\rho_G \; C_G\right)^{-\frac{1}{2}} \tag{51}$$

where "K_a" is the sonic agglomeration coefficient, and "C_G" is the speed of sound in the gas. The speed of sound of an ideal gas is given by:

$$C_G = \left(\frac{\gamma \; R \; T}{M_G}\right)^{-\frac{1}{2}} \tag{52}$$

where "γ" is the ratio of specific heats, and "R" is the universal gas constant, and "M_G" is the gas molecular weight.

Figure 13 shows the relative sonic agglomeration coefficient for a variety of temperatures and pressures. Once again, high temperatures can slightly improve agglomeration at atmospheric pressure, but high temperature and high pressure together significantly reduce sonic agglomeration relative to standard conditions.

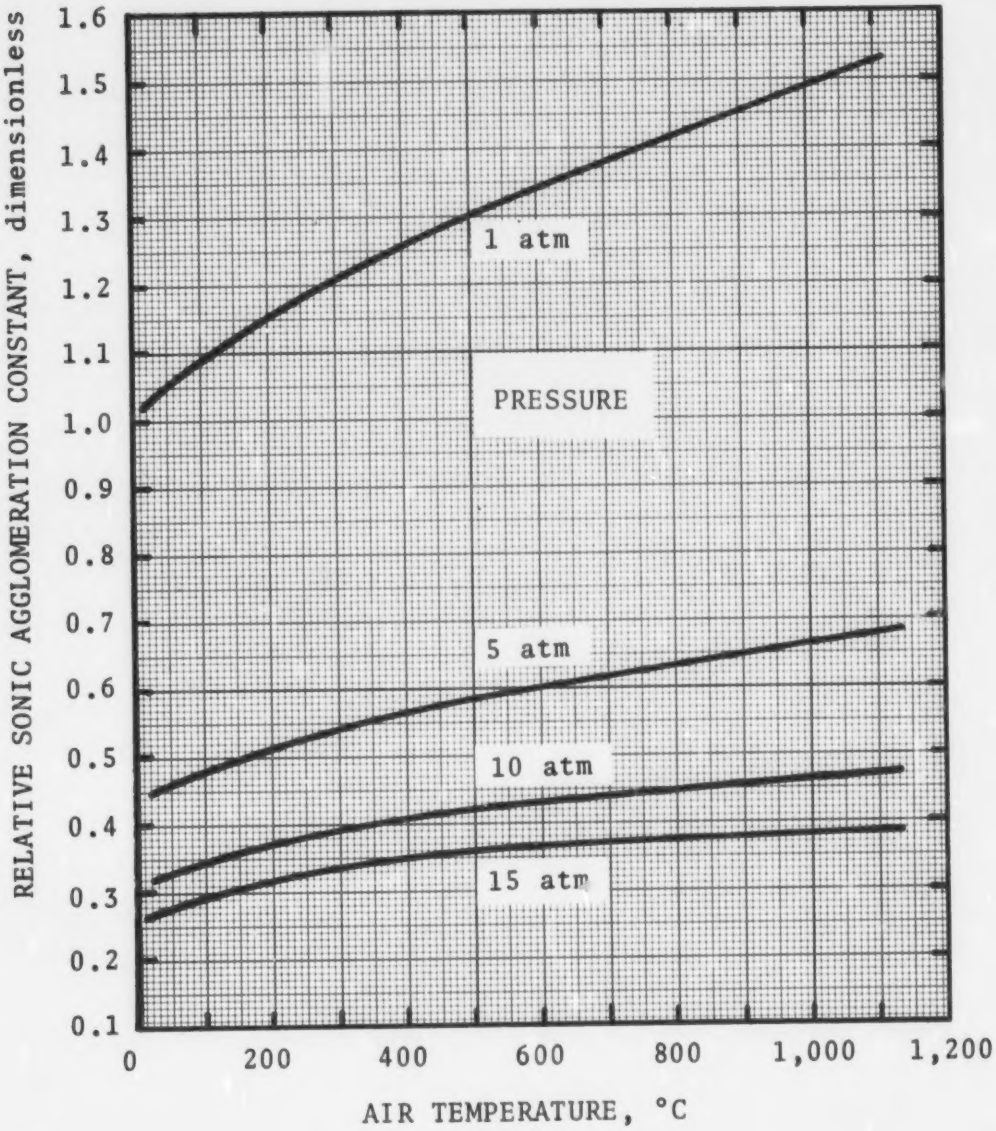

Figure 13. Sonic agglomeration of particles at high temperature and pressure.

PROPERTIES

In previous sections it has been shown that the removal of suspended particulate matter from a gas is strongly dependent on the resistance of the gas to the motion of a particle. The gas resistance force is a function of a number of gas properties, the most important of which are the absolute viscosity of the gas and the mean free path of the gas molecules. Also, but to a lesser extent, other properties such as density, thermal conductivity, and molecular diffusivity influence particle collection.

In this section, the effects of high temperature and high pressure on the important gas properties are reviewed.

ABSOLUTE VISCOSITY

The absolute viscosity of a gas is defined by Newton's law of friction:

$$\tau_G = \mu_G \frac{du}{dy} \tag{53}$$

where "τ_G" is the frictional shearing stress in the fluid, and "du/dy" is the velocity gradient perpendicular to the flow. The viscosity is thus the proportionality constant relating "τ_G" and "du/dy", and characterizes the resistance of the fluid to shearing stresses.

The absolute viscosities of gases and gas mixtures at temperatures up to 1,200°C have been studied by Saxena (1971), and experimental values are presented for many gases by Weast (1968).

Gas viscosities also can be predicted from a number of empirical equations presented and discussed by Reid and Sherwood (1958). They found the average error in these empirical equations to be about 3%. If experimental viscosity values are available at two temperatures, Reid and Sherwood (1958) recommend using the following approximation:

$$\mu_G = \frac{T^{1.5}}{mT + b} \tag{54}$$

where "T" is absolute temperature in "°K","μ_G" is in micropoise, and "m" and "b" are constants which must be obtained empirically for each gas. Figure 14 compares the theoretical curve obtained from equation (54) with experimental data from Weast (1968), for air.

Equation (54) and data from Weast (1968) were used to predict viscosity versus temperature curves for many common gases. The results are presented in Figure 15. The viscosity of water vapor increases most steeply with increasing temperature. As the temperature increases from 100°C to 1,700°C, the viscosity of water vapor increases by a factor of about 5.5. The other gases are less sensitive to temperature, with a similar temperature increase only causing the viscosity to increase by a factor of 2 to 2.5.

In practical situations, mixtures of various gases are present. The viscosity of a gas mixture can be obtained by using equations presented by Reid and Sherwood (1958) and attributed to Bromley and Wilke (1951). The calculations are quite tedious and generally are not necessary in determining the effects of temperature on the gas viscosity. Usually it is satisfactory to assume the gas viscosity will behave similar to that of air.

From simple kinetic theory it would be expected that the viscosity should not depend on pressure. In a dense gas, however, the forces of attraction and repulsion between molecules causes the viscosity to increase rapidly with pressure. This effect is especially noticeable at low temperatures. However, for air at 0°C, the viscosity is not affected significantly by pressures below about 20 atm. At 1,000°C the viscosity is independent of pressures up to about 300 atm. Therefore the effect of high pressure on the viscosity has not been considered

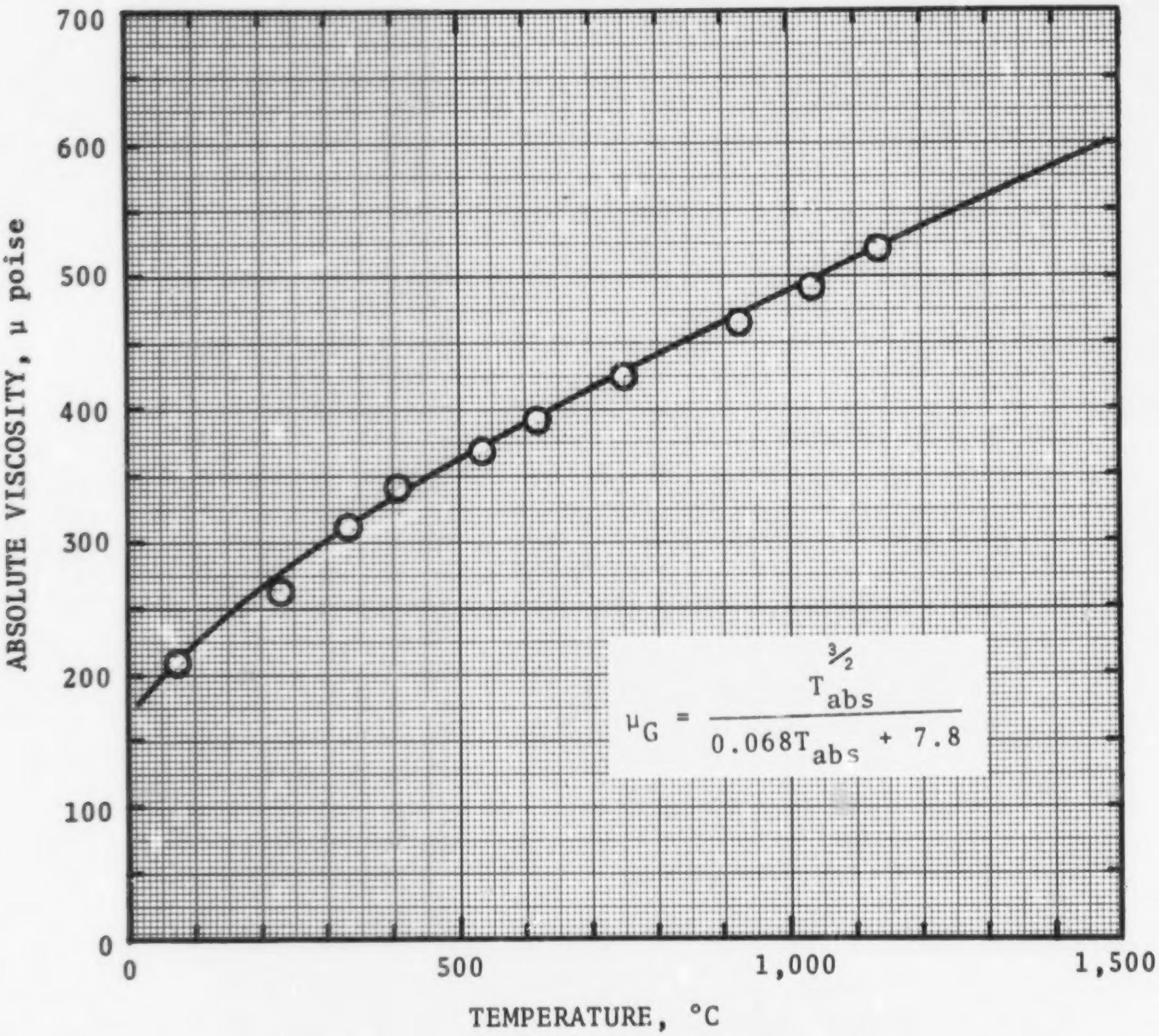

Figure 14. Experimental and theoretical viscosity versus temperature curves for air. Data from Weast (1968).

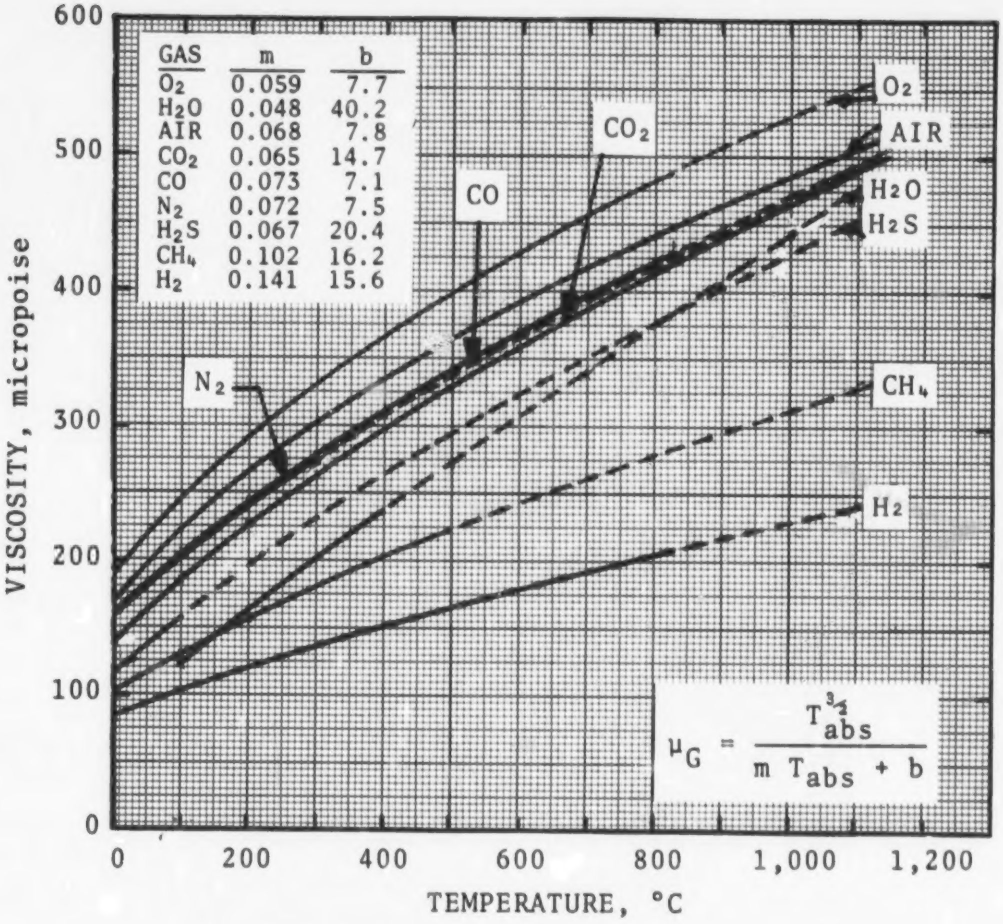

GAS	m	b
O_2	0.059	7.7
H_2O	0.048	40.2
AIR	0.068	7.8
CO_2	0.065	14.7
CO	0.073	7.1
N_2	0.072	7.5
H_2S	0.067	20.4
CH_4	0.102	16.2
H_2	0.141	15.6

$$\mu_G = \frac{T_{abs}^{3/2}}{m\ T_{abs} + b}$$

Figure 15. Gas viscosity versus temperature. The solid lines are interpolated between data, and the dashed lines are extrapolated from data. Data are from Weast (1968).

important in this study. Methods for predicting the effect of pressure on gas viscosity are presented by Reid and Sherwood (1958).

MEAN FREE PATH

The mean free path of gas molecules is defined as the average distance between molecular collisions. From the kinetic theory of gases, the mean free path, λ, is given by the Chapman-Enskog equation:

$$\lambda = \frac{\mu_G}{0.499\ \rho_G\ \bar{c}} \tag{55}$$

where "$\bar{c}$" is the root mean square molecular velocity, and is given by:

$$\bar{c} = \left(\frac{8}{\pi}\ \frac{R\ T}{M}\right)^{\frac{1}{2}} \tag{56}$$

Making use of the ideal gas law and equation (56), equation (55) becomes:

$$\lambda = \frac{\mu_G}{0.499\ P}\left(\frac{\pi}{8}\ \frac{R\ T}{M}\right)^{\frac{1}{2}} \tag{57}$$

If the mean free path for a gas is known at one temperature and pressure, its value at any other temperature and pressure can be obtained using the formula:

$$\frac{\lambda}{\lambda_o} = \frac{\mu_G}{\mu_o}\ \frac{P_o}{P}\left(\frac{T}{T_o}\right)^{\frac{1}{2}} \tag{58}$$

where the subscript "o" denotes values at the known conditions. The mean free path of air molecules is presented as a function of temperature and pressure in Figure 16.

The mean free paths for mixtures found in actual process effluent gases can be obtained from equations (57) and (58) if the molecular weight and viscosity of the gas mixture are known.

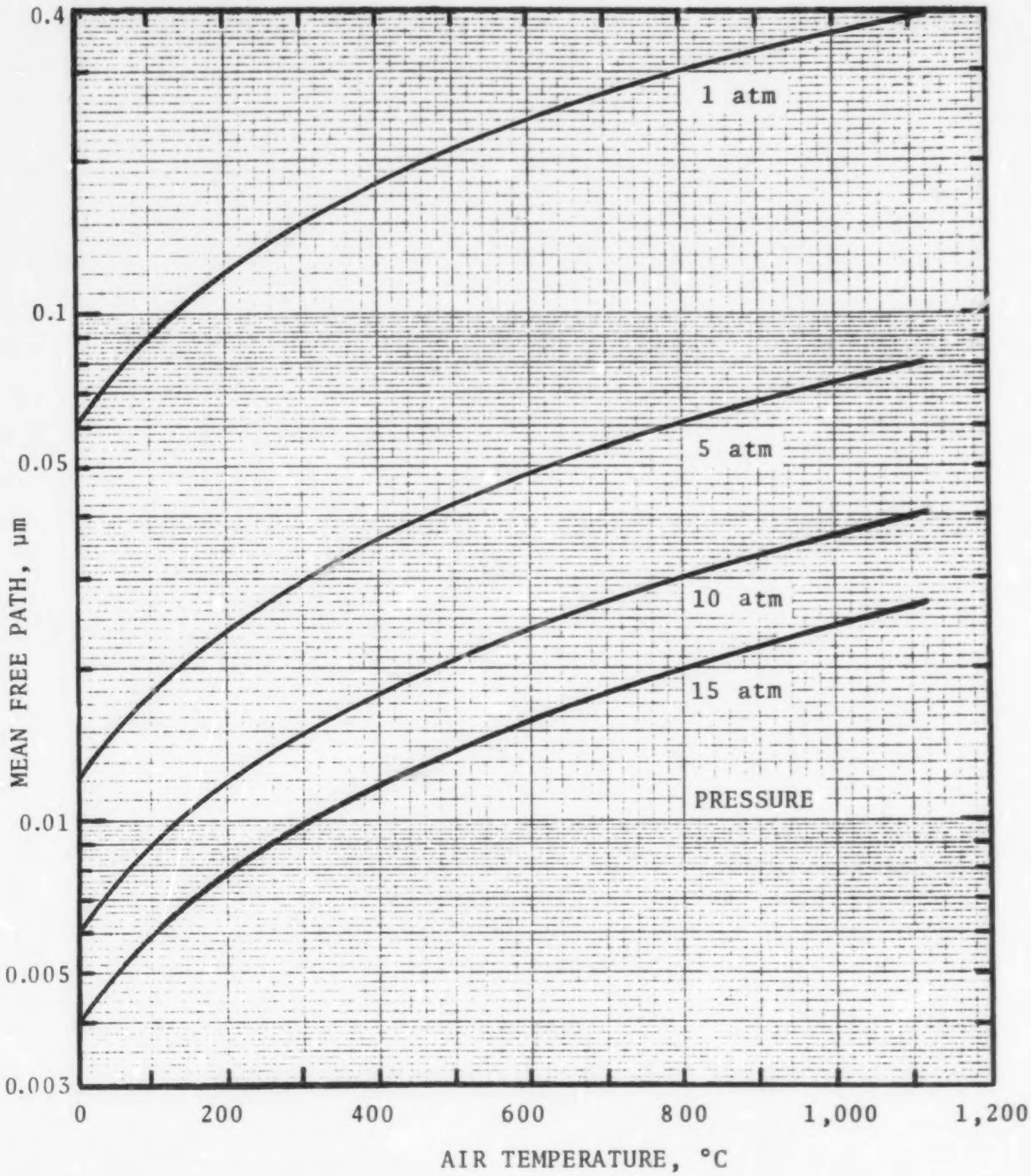

Figure 16. Mean free path of air molecules as a function of temperature and pressure.

GAS DENSITY

For a perfect gas, the density of the gas is related to the temperature and pressure through the equation of state:

$$\rho_G = \frac{M_G P}{R\ T} \tag{59}$$

This expression is suitable at high temperatures and pressures providing that the gas still acts like a perfect gas. If the pressure is large enough, the compressibility of the gas becomes important and equation (59) must be modified by a compressibility factor which is itself a function of temperature and pressure. Equation (59) is suitable up to about 20 atm pressure at 0°C and up to over 300 atm at temperatures larger than 1,000°C. The use of compressibility factors is discussed by Reid and Sherwood (1958) and most general thermodynamics textbooks.

THERMAL CONDUCTIVITY

The collection of particles by the mechanism of thermophoresis depends on the ratio of the thermal conductivities of the gas and the particle. The thermal conductivity, k_t, of a substance is defined by:

$$Q_x = - k_t \frac{\partial T}{\partial x} \tag{60}$$

where "Q_x" is the heat flux in the "x" direction, and "T" is the temperature. Thus the thermal conductivity characterizes the rate of heat transfer through a substance.

The thermal conductivity of gases is a function of the specific heat and the viscosity of the gas, and hence is a function of temperature. It is not a significant function of pressure for pressures below about 15 atm.

Experimental investigations of the thermal conductivity of gases and gas mixtures have been conducted by Saxena (1971, 1972) and by Chen and Saxena (1973). Also Reid and Sherwood (1958) present empirical equations and some data for thermal conductivity as a function of temperature and pressure.

Both the viscosity and the specific heat are functions of temperature. The constant pressure specific heat for air is presented as a function of temperature in Figure 17. This was taken from a nomograph presented by Liley (1963).

Gambill (1963) presents a relatively simple empirical expression relating the thermal conductivity, k_G, to the gas viscosity and specific heat, expressed in English units as shown:

$$k_G(\text{BTU/hr-ft-°F}) = \mu_G(\text{lb/hr-ft}) \left[C_p(\text{BTU/lb-°F}) + \frac{2.48}{M_G} \right] \qquad (61)$$

where "M_G" is the molecular weight of the gas. Equation (61) and Figure 17 were used to determine the thermal conductivity of air as a function of temperature. The results are presented in Figure 18 together with the experimental data obtained by Saxena (1973) for nitrogen.

The thermal conductivities of other gases may be approximated in a similar manner using equation (61), or may be estimated by more elaborate methods described by Reid and Sherwood (1958), by Gambill (1963), and by Saxena (1971).

The thermal conductivity of solid particles, k_p, may be predicted from equations presented by Gambill (1963), however the temperature dependence of the thermal conductivity of materials likely to be found in fly ash (Fe_2O_3, SiO_2, Al_2O_3) is quite small. Therefore the temperature dependence of the gas to particle thermal conductivity ratio will depend primarily on the thermal conductivity of the gas.

Figure 18 indicates that the ratio of "k_G/k_p" will increase by a factor of 3 if the temperature is increased from 0°C to 1,100°C.

MOLECULAR DIFFUSIVITY

Particle collection by diffusiophoresis involves the molecular diffusivity of the vapor in the gas. The rate of molecular transfer, N_A, in molal units per unit area in unit time is given by Fick's law:

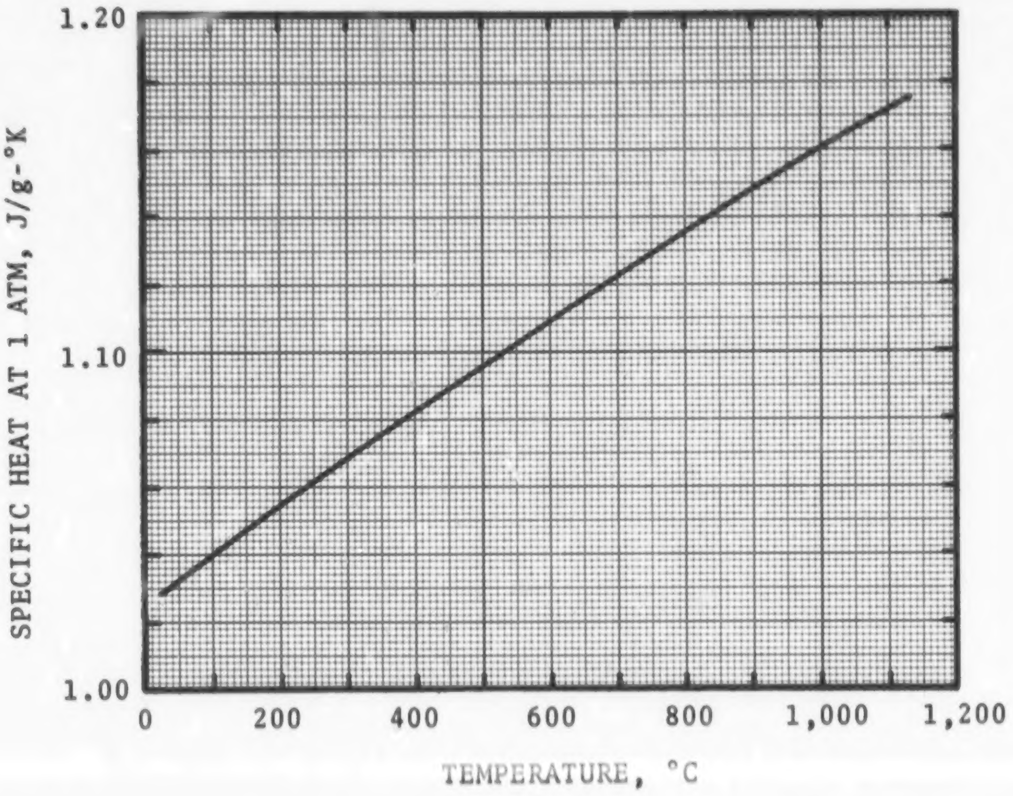

Figure 17. Specific heat as a function of temperature for air at 1 atm. From nomograph presented by Liley (1963).

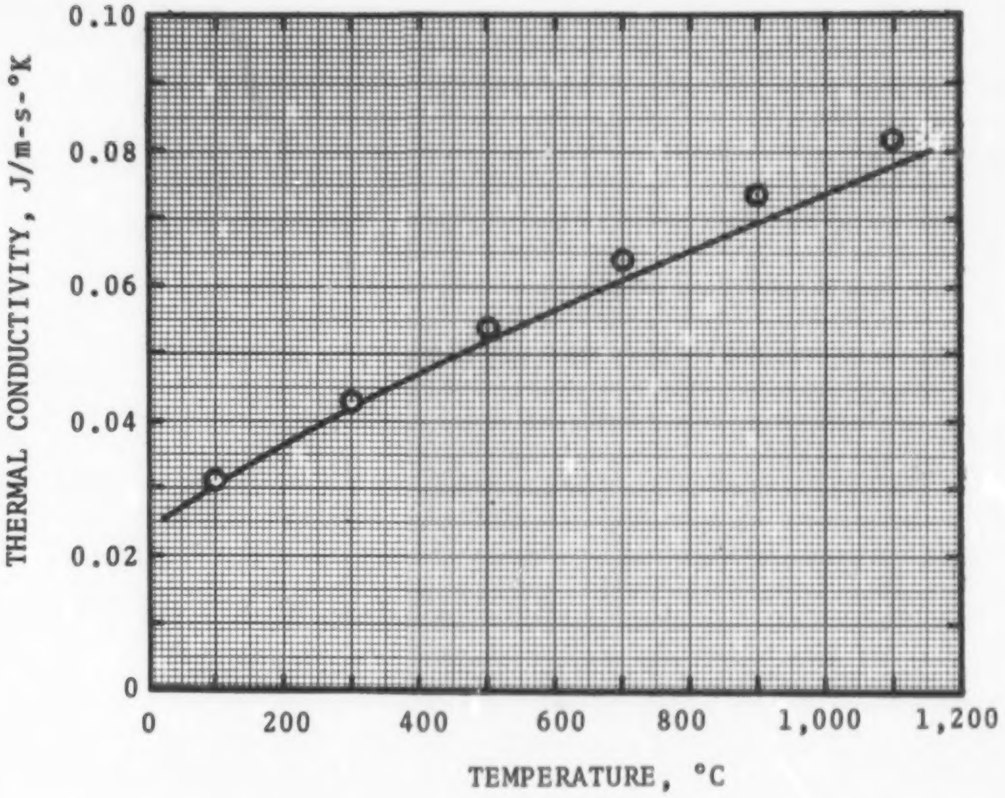

Figure 18. The effect of temperature on the thermal conductivity of air at 1 atm pressure.
(0.58 x J/m-s-°K = BTU/hr-ft-°F)
Data from Saxena (1973), for N_2

$$N_A = - D_{vG} \frac{dc_A}{dx} \qquad (62)$$

where "dc_A/dx" is the concentration gradient in the direction of diffusion, and "D_{vG}" is the molecular diffusivity or diffusion coefficient of the vapor in the gas.

The molecular diffusivity can be calculated from a number of empirical equations presented by Reid and Sherwood (1958), and in general they predict:

$$D_{vG} \propto \frac{T^{3/2}}{P} \qquad (63)$$

Reid and Sherwood (1958) state that the product "$D_{vG} \cdot P$" is constant for a given temperature for pressures up to 20-25 atm.

They also present data for the diffusion coefficients of water vapor in air, at 1 atm pressure, for temperatures up to 1,200°C. These data are plotted in Figure 19. The dashed line is the prediction based on equation (63) and the experimental diffusivity at T=100°C. Thus equation (63) underestimates the temperature dependence of "D_{vG}".

THERMAL EXPANSION

The thermal expansion of particles at high temperature will increase their size and could thereby improve the collection efficiency of devices operating at high temperature.

Most fly ash is composed of refractory material such as silica and alumina. Monroe (1963) presents data for the thermal expansion of refractory materials, and the data for silica brick are reproduced in Figure 20. The thermal expansion increases with temperature up to about 700°C, and then remains constant at higher temperatures. The maximum expansion is only about 1.5%, and therefore the increase in size of a particle at high temperature is expected to be negligible.

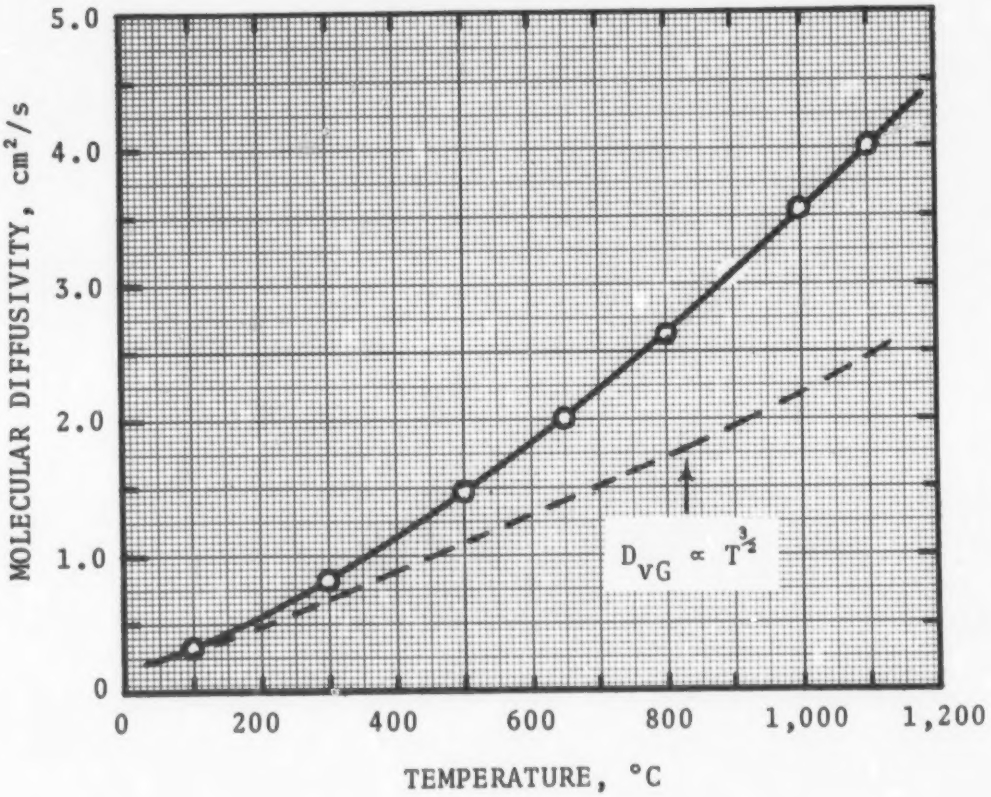

Figure 19. Molecular diffusivity of water vapor in air as a function of temperature. Data from Reid and Sherwood (1958).

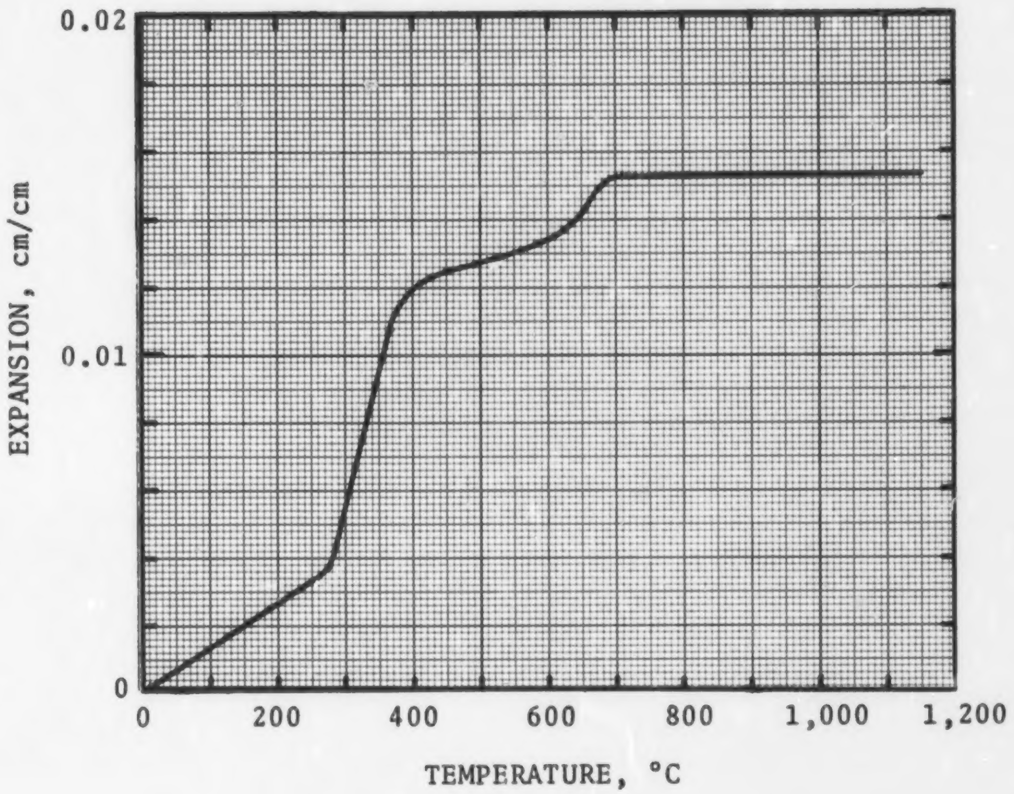

Figure 20. The thermal expansion of silica brick at high temperatures. From Monroe (1963).

EXAMPLE APPLICATIONS

In most particle collection devices, many collection mechanisms are acting simultaneously. Often one mechanism dominates, as in electrostatic precipitation, and the deposition velocity resulting from this mechanism can be used to characterize the collection efficiency of the device. Sometimes, however, many mechanisms are important and they must be combined, as in fiber filtration, in order to characterize the device.

In this section, therefore, a few examples of the effects of high temperature and pressure on the theoretical efficiencies of particle collection devices (specifically: a cyclone separator, a fiber filter, and a granular bed filter) are presented. We have not attempted to critically review the theoretical models used in this section. We have taken typical models from the literature, which are based on the basic mechanisms discussed in a previous section above, and used them to predict the efficiencies at high temperature and pressure. Our purpose in presenting these examples is to provide an indication of the relationship between the fundamental mechanisms and collection devices.

Because particle collection equipment usually is necessary in order to meet the air pollution emissions standards, perhaps a more important consideration is the amount of power required to maintain a high collection efficiency for a given device. The first example presented in this section, therefore, considers the power requirement for one of the most important collection mechanisms, inertial impaction.

SINGLE STAGE IMPACTOR

Using equation (4) to represent the fluid resistance force, it is possible to predict the collection efficiency and work requirements for particle collection by inertial impaction. Figure 21 shows the particle cut diameter as a function of flow work (or specific power) for a single stage impactor at various temperature and pressure conditions. For an impactor, it may be

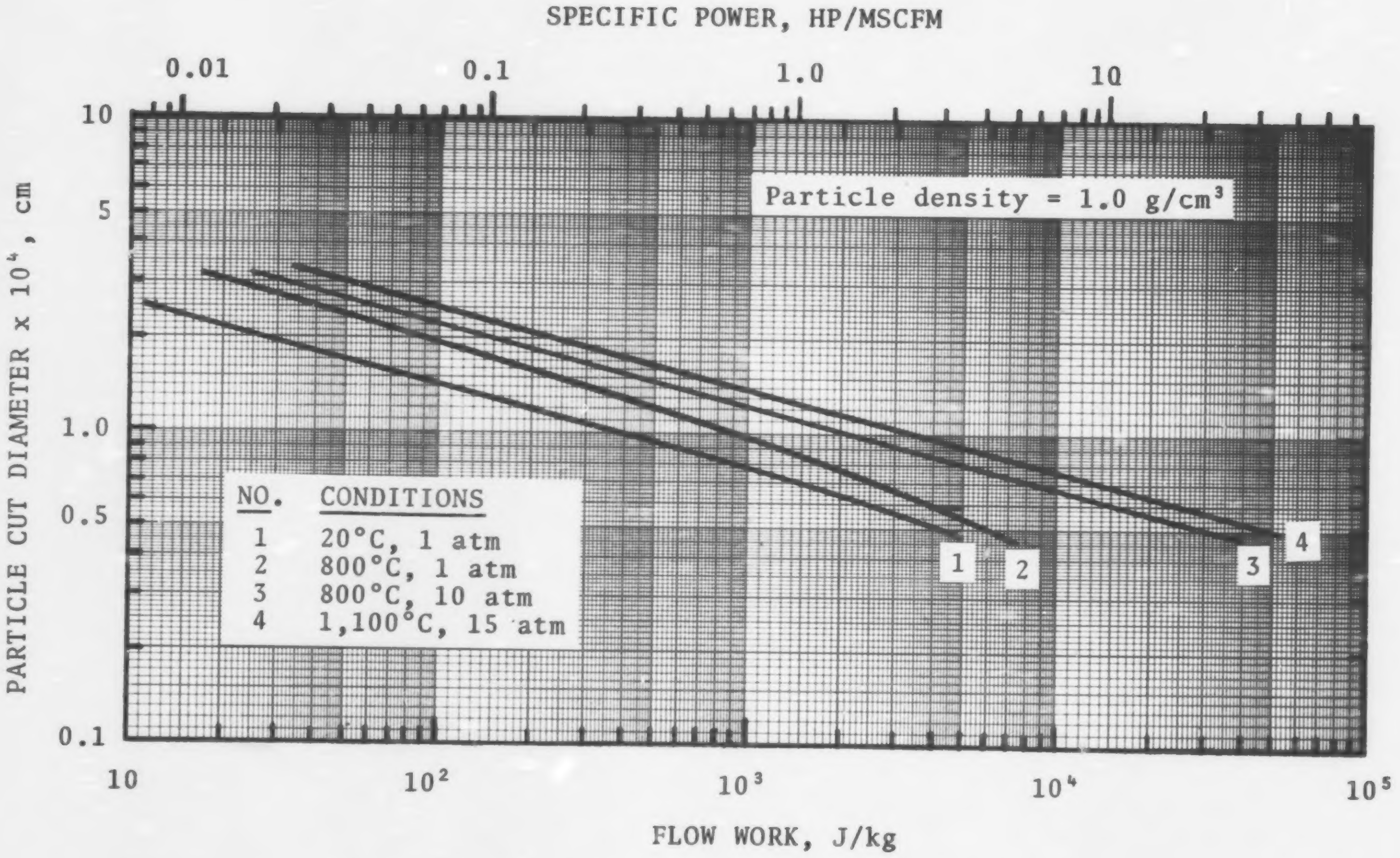

Figure 21 . Flow work (specific power) for impaction from a round jet as a function of temperature and pressure.

assumed that all particles larger than the cut diameter will be collected. The flow work is equivalent to the energy requirement per mass of gas. The power requirement would be equal to the flow work multiplied by the mass flow rate.

Figure 21 illustrates that the work required to collect submicron particles by inertial impaction increases rapidly with decreasing particle diameter. The effects of temperature and pressure may be seen by comparing the four curves. Curve 1 represents standard temperature and pressure conditions. Curve 2 shows the effect of high temperature at atmospheric pressure. The work required to collect submicron particles does not increase as rapidly as that required to collect larger particles. The reason for this is that, for a given particle diameter, the fluid resistance force decreases as the mean free path of the gas molecules increases. The mean free path increases with temperature, for a constant pressure.

Curves 3 and 4 are for simultaneous high pressure and high temperature conditions. The beneficial effect of high temperature on the mean free path is completely nullified by a decrease in mean free path with increasing pressure. The work required to remove submicron particles is greatly increased. For example, the collection of all particles greater than 1 μm by inertial impaction would require about 450 J/kg (0.31 HP/MSCFM) at standard conditions (Curve 1). It would require about 4,000 J/kg (2.8 HP/MSCFM) at 1,100°C and 15 atm (Curve 4). This is equivalent to approximately a 9:1 increase in the power requirement to maintain a similar degree of particle removal.

CYCLONE SEPARATOR EFFICIENCY

A further illustration of the effect of high temperature and pressure on particle collection may be obtained by predicting the collection efficiency of a cyclone separator operating at various temperatures and pressures, for the same inlet velocity.

Leith and Licht (1972) derived an equation for predicting cyclone efficiency from theoretical considerations (this work is reported by Calvert et al. (1972). Their equation is:

$$E = 1 - \exp\left[-2\,(C\Psi)^{1/(2n+2)}\right] \qquad (64)$$

where "C" is a function of the cyclone dimension ratios only. The temperature and pressure dependent terms are contained in the modified inertial parameter, Ψ, and the vortex exponent, n, defined by:

$$\Psi = \frac{\rho_p\, d_p^2\, u_G}{18\, \mu_G\, D_c}\,(n+1) \qquad (65)$$

and:

$$n = 1 - \left(1 - \frac{(0.00394\, D_c)^{0.14}}{2.5}\right)\left(\frac{T}{283}\right)^{0.3} \qquad (66)$$

where "D_c" is the cyclone diameter, "u_G" is the gas velocity, and "T" is absolute temperature.

Equations (64), (65), and (66) were used to calculate typical collection efficiency curves for a high efficiency cyclone. The cyclone was assumed to be about 15 cm (6 inches) in diameter with a volumetric flow rate of about 1.4 m^3/min (50 ft^3/min).

Figure 22 shows a typical efficiency curve for a high efficiency cyclone (Curve 1). The cyclone cut point (50% efficiency) occurs at a particle diameter of about 1 μm, and the cyclone is better than 99% efficient for particles larger than 15 μm.

Curve 2 shows the estimated cyclone efficiency for a gas at 1,100°C and atmospheric pressure, and for the same inlet gas velocity as in Curve 1. The cyclone efficiency has dropped significantly and now has a cut point occurring at 2.0 μm and is only 96% efficient for 15 μm particles.

Curve 3 shows the estimated cyclone efficiency for a gas at 1,100°C and 15 atm, for the same inlet velocity. The cyclone efficiency has decreased again slightly for small particles, but is relatively unaffected for larger particles. The cut point now occurs at 2.5 μm and the efficiency for 15 μm particles is 95%.

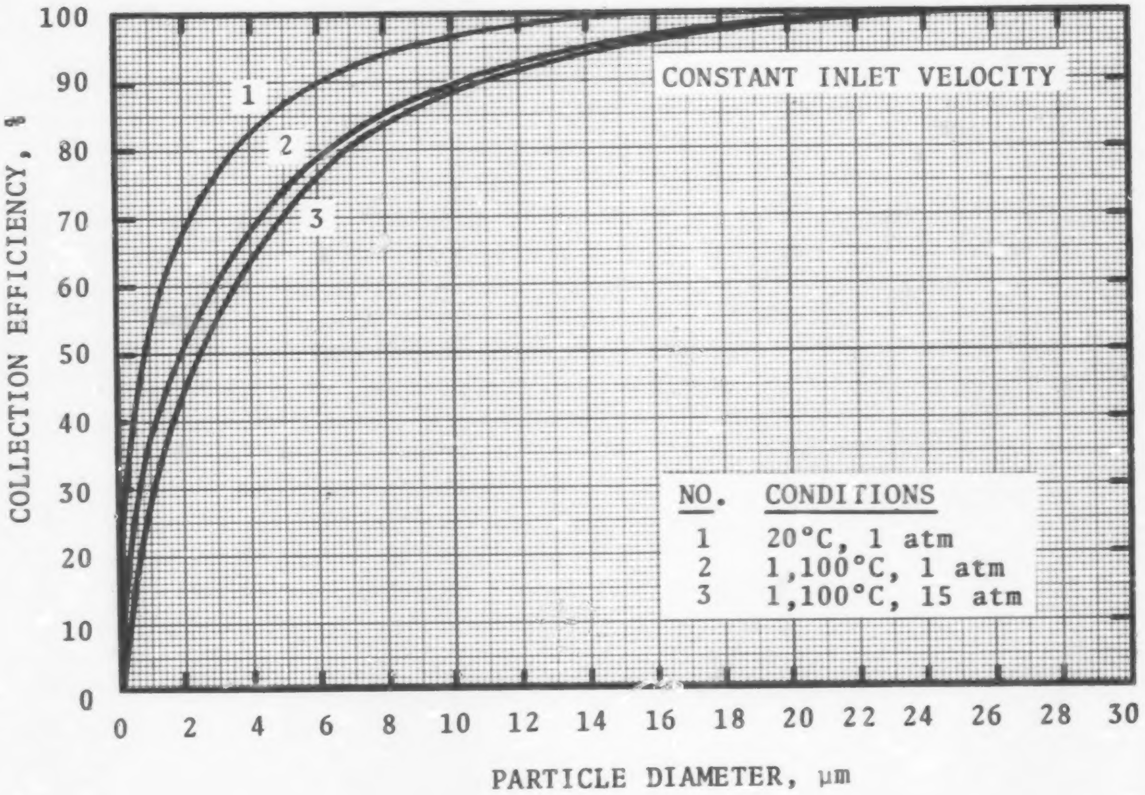

Figure 22. The effects of high temperature and pressure on the collection efficiency of a high efficiency cyclone.

SPECIFIC POWER FOR A CYCLONE SEPARATOR

Figure 23 presents another example of high temperature and pressure effects on the performance of a cyclone separator. The specific power ratio is the ratio of the specific power (HP/MSCF) at high temperature and pressure to that at standard conditions. The curves in Figure 23 show the power requirement relative to standard conditions to collect various particle sizes while maintaining a constant collection efficiency for each particle size.

EFFICIENCY OF A FIBER BED

Figure 24 shows the effects of temperature and pressure on the collection efficiency of a fiber bed. The curves were calculated from the theory presented by Calvert et al. (1972) and attributed to Torgeson (1958). The collection efficiency is the combined efficiency resulting from inertial impaction, interception, and Brownian diffusion.

From Figure 24 it is apparent that the filter collection efficiency for particles larger than about 0.5 μm in diameter is reduced significantly at high temperature and pressure. This is a result of the smaller inertial impaction parameter [equation (2)] at high temperature and pressure. For particles smaller than 0.5 μm, the collection efficiency is somewhat increased because of the increased Brownian motion at high temperatures.

At high temperature and atmospheric pressure the collection efficiency is greatly increased for particle diameters up to about 0.9 μm. For particles larger than 1 μm the collection efficiency is reduced at high temperature and atmospheric pressure, although not as severely as at high temperature and high pressure.

COLLECTION EFFICIENCY OF A GRANULAR BED

No generally accepted theory is available for the detailed design of granular bed filters, especially for high temperature and pressure applications.

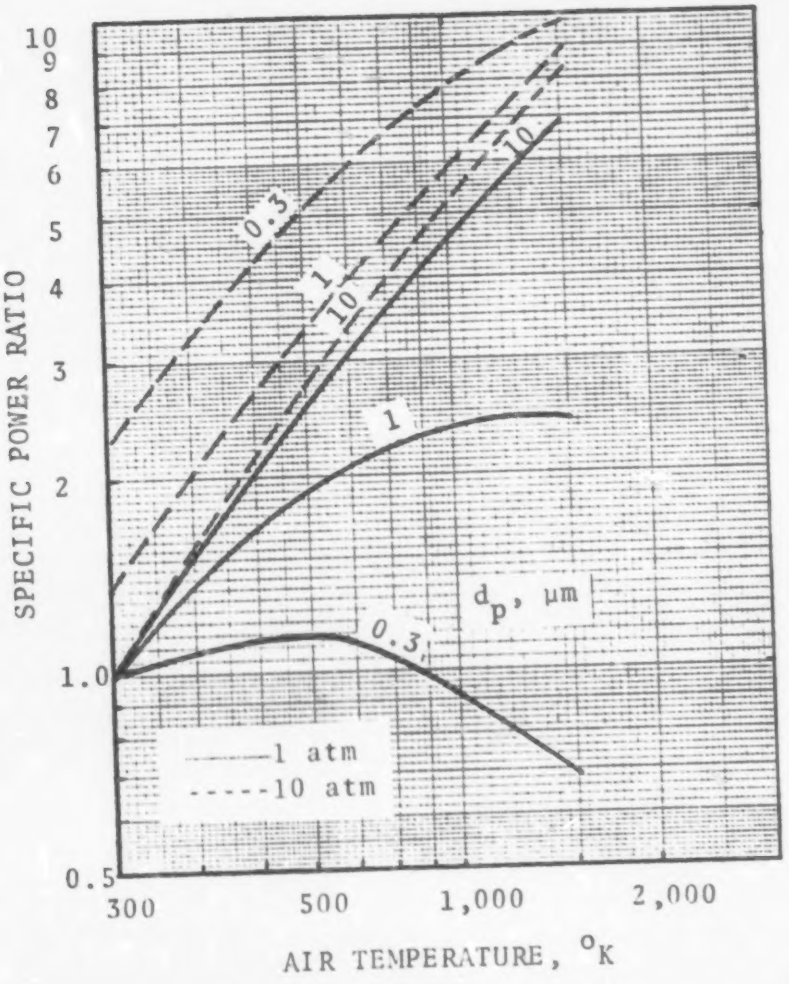

Figure 25. The specific power requirements for a cyclone as a function of temperature and pressure.

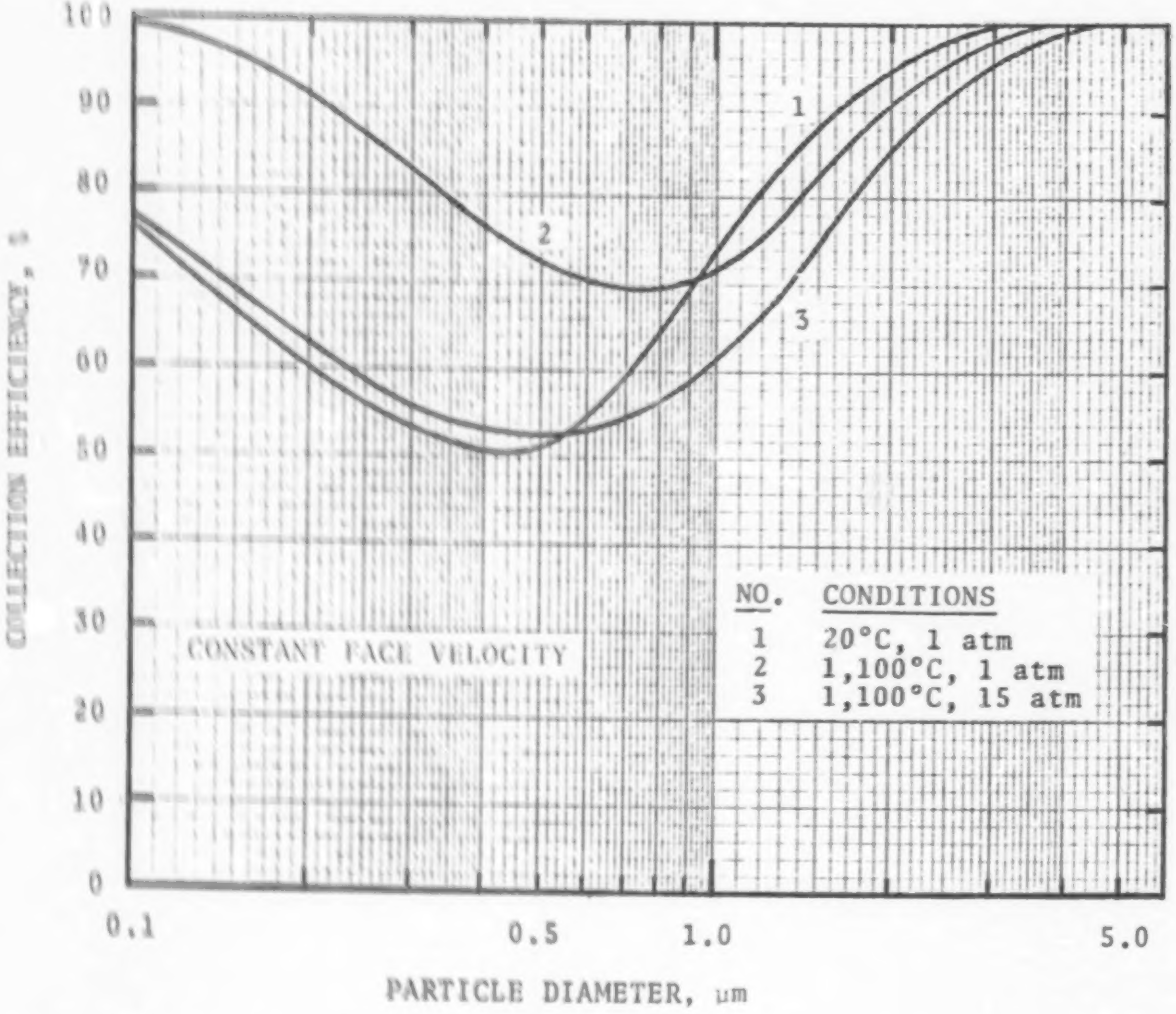

Figure 24. The effects of high temperature and pressure on the collection efficiency of a fiber bed.

A simple model for particle penetration was developed by Calvert, et al. (1972) and correlated with experimental data on collection of particles in packed beds. This model may be used to predict the efficiency of granular beds. Actual efficiencies may be higher if a filter cake is formed, or if significant agglomeration, diffusion, or thermal deposition is present.

Penetration through packed spherical collectors may be approximated by:

$$Pt = \exp - \left[21.4 \frac{Z}{d_c} K_p \right] \tag{67}$$

where "Z" is the bed depth, "d_c" is the collector diameter, and "K_p" is the inertial impaction parameter. In this case, "K_p" is defined as:

$$K_p = \frac{u_f \; d_p^2 \; C' \; \rho_p}{9 \; \mu_G \; d_c} \tag{68}$$

where "u_f" is the gas velocity based on empty cross-sectional area (superficial velocity).

The collection efficiency of a granular bed, as a function of temperature, pressure, and particle diameter, is shown in Figure 25. It is assumed that the bed is 0.04 m deep, the collectors are 0.002 m in diameter, the particle density is 2,500 kg/m³ (2.5 g/cm³), the superficial velocity is 1 m/s, and the gas is air.

Because this model is based primarily on inertial impaction, the increase in collection efficiency at high temperature and small particle diameter is the result of the decreased drag force at larger mean free paths. Diffusion would further increase the collection efficiency for small particles, especially at high temperature.

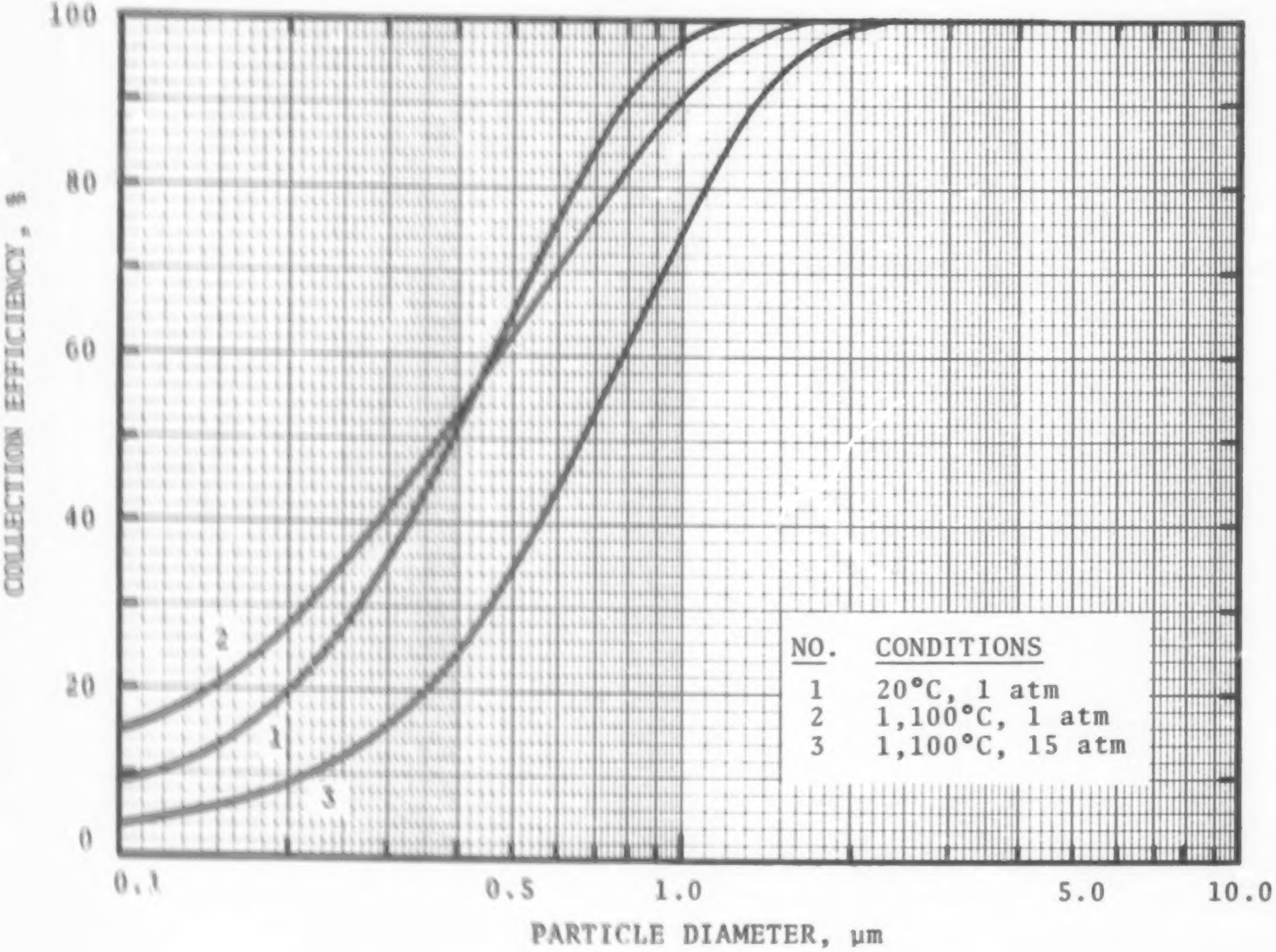

Figure 28. The effects of high temperature and pressure on the inertial collection efficiency of a packed bed.

BIBLIOGRAPHY

Beal, S.K. Turbulent Agglomeration of Suspensions. J. Aerosol Science, 3: 113, 1972.

Billings, C.E., W.D. Small, and L. Silverman. Pilot-Plant Studies of a Continuous Slag-Wool Filter for Open-Hearth Fume. A.P.C.A. Journal, 5 (3): 159, 1955.

Billings, C.E., L.N. Levenbaum, C. Kurker, Jr., E.C. Hickey, and L. Silverman. Further Investigations of the Continuous Slag-Wool Filter. A.P.C.A. Journal, 8 (1): 53, 1958a.

Billings, C.E., C. Kurker, Jr., and L. Silverman. Simultaneous Removal of Acid Gases, Mists, and Fumes with Mineral Wool Filters. A.P.C.A. Journal, 8 (3): 185, 1958b.

Billings, C.E., L. Silverman, R. Dennis, and L.H. Levenbaum. Shock Wave Cleaning of Air Filters. A.P.C.A. Journal, 10 (4): 318, 1960.

Brock, J.R. On the Theory of Thermal Forces Acting on Aerosol Particles. J. Colloid Sci., 17: 768, 1962.

Bromley, L.A., and C.R. Wilke. Ind. Eng. Chem., 43: 1641, 1951.

Brown, R.F., and A.B. Walker. Feasibility Demonstration of Electrostatic Precipitation at 1700°F. A.P.C.A. Journal, 21 (10): 617, 1971.

Byers, R.L., and S. Calvert. Particle Deposition from Turbulent Streams by Means of Thermal Force. Ind. Eng. Chem. Fundamentals, 8 (4): 646, 1969.

Calvert, S., J. Goldshmid, D. Leith, and D. Mehta. Scrubber Handbook. A.P.T., Inc. EPA-R2-72-118a, NTIS: PB 213016, August 1972.

Calvert, S., J. Goldshmid, D. Leith, and N.C. Jhaveri. Feasibility of Flux Force/Condensation Scrubbing for Fine Particulate Collection. EPA-650/2-73-036, October 1973.

Chen, S.H.P., and S.C. Saxena. Experimental Determination of Thermal Conductivity of Nitrogen in the Temperature Range 100-2200°C. High Temp. Sci., 5: 206, 1973.

Cunningham, E. Proc. Roy Soc. (London), A83: 357, 1910.

Davies, C.N. Definitive Equations for the Fluid Resistance of Spheres. Proc. Phys. Soc. 57 (4): 18, July 1945.

Derjaquin, B.V., and Y. I. Yalamov. The Theory of Thermophoresis and Diffusiophoresis of Aerosol Particles, in Int'l Rev. Aerosol Phys. Chem., Vol. 3, ed. G.M. Hidy and J.R. Brock, Pergamon Press, New York, 1972.

Epstein, P.S. Zur Theorie des Radiometers. Z. Phys., 54: 537, 1929.

First, M.W., J.B. Graham, G.M. Butler, C.B. Walworth, and R.P. Warren. High Temperature Dust Filtration. Ind. Eng. Chem. 48 (4): 696, 1956.

Fuchs, N.A. Evaporation and Droplet Growth in Gaseous Media. Pergamon Press, N.Y., 1959.

Fuchs, N.A., The Mechanics of Aerosols. Pergamon Press, N. Y., 1964.

Gambill, W.R., Prediction and Correlation of Physical Properties, in Perry's Chemical Engineer's Handbook, Section 3, McGraw-Hill, N. Y., 1963.

Goodman, F.O., and H.Y. Wachman. Formula for Thermal Accommodation Coefficients. J. Chem. Phys. 46 (6): 2376, 1967.

Goodman, F.O. Classical Theory of Small Energy Accommodation Coefficients. J. Chem. Phys. 50 (9): 3855, 1969.

Green, H.L., and W.R. Lane. Particulate Clouds: Dusts, Smokes and Mists. D. Van Nostrand Co., N.Y. 1964.

Gussman, R.A., and A.M. Sacco. Aerosol Behavior in High Pressure Environments. Report No. 1894, U.S. Dept. of the Navy, February 1970.

Hidy, G.M., and J.R. Brock. The Dynamics of Aerocolloidal Systems. Pergamon Press, N.Y., 1970.

Kane, L.J., G.E. Chidester, and C.C. Shale. Ceramic Fibers for Filtering Dust from Hot Gases. Bur. of Mines, Report of Investigations, 5672, 1960.

Koller, L.R., and H.A. Fremont. Negative Wire Corona at High Temperature and Pressure. J. Appl. Phys. 21: 741, 1950.

Kornberg, J.P. High Temperature Filtration of Particulates by Diffusion. Doctoral Thesis, Harvard School of Public Health, Boston, Mass., 1973.

Lapple, C.E., and C.B. Shepherd. Calculation of Particle Trajectories. Ind. Eng. Chem. 32 (5): 605, 1940.

Leith, D., and W. Licht. Collection Efficiency of Cyclone Type Particle Collectors, a New Theoretical Approach. A.I.Ch.E. Symp. Series: Air, 1971.

Liley, P.E. Physical and Chemical Data, in Perry's Chemical Engineer's Handbook, Section 3, McGraw-Hill, N.Y., 1963.

Lundgren, D.A., and T.C. Gunderson. Filtration Characteristics of Glass Fiber Filter Media At Elevated Temperatures. E.P.A.-600/2-76-192, O.R.D., R.T.P., N.C., July 1976.

Mašek, V. Über die Temperatur - und Frequenz -abhängigkeit der dielektrishen Eigenschaften von Kokerei-Flugstaub. Staub-Reinhalt. Luft, 33 (12): 479, 1973.

Matlosz, R.L., S. Leipziger, and T.P. Torda. Investigation of Liquid Drop Evaporation in a High Temperature and High Pressure Environment. Int. J. Heat Mass Transfer, 15: 831, 1972.

Maxwell J. Collected Scientific Papers, Cambridge, 1890.

Mednikov, E.P. Acoustic Coagulation and Precipitation of Aerosols. Consultant Bureau, N.Y., 1965.

Millikan, R.A. Coefficients of Slip in Gases and the Law of Reflection of Molecules from the Surfaces of Solids and Liquids. Phys. Rev. 21 (3): 217, 1923a.

Millikan, R.A. The General Law of Fall of a Small Spherical Body Through a Gas, and its Bearing upon the Nature of Molecular Reflection from Surfaces. Phys. Rev. 22 (1):1, 1923b.

Monroe, E.S. Combustion-Equipment Design: In Perry's Chemical Engineer's Handbook, Section 9, McGraw Hill, New York, 1963.

Morley, W.J., and J.C. Wisdom. Brown Coal Ash Deposition in the Open-Cycle Gas Turbine. J. Inst. Fuel, 187, May 1964.

Parent, J.D. Efficiency of Small Cyclones as a Function of Loading, Temperature and Pressure Drop. Trans. A.S.Ch.E. 42: 989, 1946.

Ramesh, V., and D.J. Marsden. Rotational and Translational Accommodation Coefficients of Nitrogen on Nickel, Silver, and Gold. Vacuum, 24 (7): 291, 1974.

Rao, A.K., M.P. Schrag, and L.J. Shannon. Particulate Removal from Gas Streams at High Temperature/High Pressure. E.P.A. 600/2-75-020, U.S. EPA., O.R.D., Wash. D.C., 1975.

Reid, R.C. and T.K. Sherwood. The Properties of Gases and Liquids. McGraw-Hill, N.Y., 1958.

Robinson, M. The Corona Threshold for Coaxial Cylinders in Air at High Pressures. I.E.E.E. Trans. on Power Apparatus and Systems, PAS-86 (2): 185, 1967.

Robinson, M. Critical Pressures of the Positive Corona Discharge Between Concentric Cylinders in Air. J. Appl. Phys. 40 (13): 5107, 1969.

Saxena, S.C. Transport Properties of Gases and Gaseous Mixtures at High Temperatures. High Temp. Sci. 3: 168, 1971.

Saxena, S.C. Determination of Thermal Conductivity of Gases by Shock-Tube Studies. High Temp. Sci. 4: 517, 1972.

Schlichting, H. Boundary-Layer Theory. McGraw-Hill, N.Y., 1968.

Shale, C.C., W.S. Bowie, J.H. Holden, and G.R. Strimbeck. Feasibility of Electrical Precipitation at High Temperatures and Pressures. Bur. of Mines Report of Investigations, 6325, 1963.

Shale, C.C., W.S. Bowie, J.H. Holden, and G.R. Strimbeck. Characteristics of Positive Corona for Electrical Precipitation at High Temperatures and Pressures. Bur. of Mines Report of Investigation, 6397, 1964.

Shale, C.C. The Physical Phenomena Underlying the Negative and Positive Coronas in Air at High Temperatures and Pressures. I.E.E.E. Int. Conv. Record, 1965.

Shale, C.C. Progress in High Temperature Electrostatic Precipitation. A.P.C.A. Journal, 17 (3): 159, 1967.

Shale, C.C. Operating Characteristics of a High Temperature Electrostatic Precipitator. Bur. of Mines Report of Investigation, 7276, 1969.

Silverman, L. Technical Aspects of High Temperature Gas Cleaning for Steel Making Processes. Air Repair, 4 (4): 189, 1955.

Snyder, C.A., and R.T. Pring. Design Considerations in Filtration of Hot Gases. Ind. Eng. Chem. 47 (5): 960, 1955.

Spaite, P.W., D.G. Stephen, and A.H. Rose, Jr. High Temperature Fabric Filtration of Industrial Gases. A.P.C.A. Journal, 11: 243, 1961.

Spurny, K., J. Hrbek, and J.P. Lodge, Jr. Analytical Methods for for Determination of Aerosols by Means of Membrane Ultrafilters XVIII. Aerosol Sampling Under Extreme Gas Conditions. Coll. Czech. Chem. Comm. 36: 2749, 1971.

Stickney, R.E. Momentum Transfer between Gas Molecules and Metallic Surfaces in Free Molecule Flow. Physics of Fluids, 5 (12): 1617, 1962.

Strauss, W. Industrial Gas Cleaning. Pergamon Press, N.Y., 1966.

Strauss, W., and B.W. Lancaster. Prediction of Effectiveness of Gas Cleaning Methods at High Temperatures and Pressures. Atmospheric Environment, 2: 135, 1968.

Tassicker, O.J. Uber die Temperatur-und Frequenzabhängigkeit der Dielektrizitätskonstante von Kraftwerksstaub. Staub-Reinhalt. Luft, 31 (8): 331, 1971.

Thomas, J.B., and E. Wong. Experimental Study of DC Corona at High Temperatures and Pressure. J. Appl. Phys. 29 (8): 1226, 1958.

Thring, M.W., and W. Strauss. The Effect of High Temperatures on Particle Collection Mechanisms. Trans. Instn. Chem. Engrs. 41: 248, 1963.

Torgeson, W.L. In General Mills Report No. 1890, Upper Atmospheric Monitoring Program, A.E.C. Contr. No. AT(11-1)-401, 1958.

Wachman, H.Y. The Thermal Accommodation Coefficient: A Critical Survey. A.R.S. Journal, 32:2, 1962.

Wachman, H.Y. Thermal Accommodation Coefficients of Helium on Tungsten at 325°, 403°, and 473°K. J. Chem. Phys. 45 (5): 1532, 1966.

Weast, R.C., ed. Handbook of Chemistry and Physics, 49th ed. The Chemical Rubber Co., Cleveland, Ohio, 1968.

White, H.J. Industrial Electrostatic Precipitation. Addison-Wesley Pub. Co., Reading, Mass., 1963.

Willeke, K. Temperature Dependence of Particle Slip in a Gaseous Medium. J. Aerosol Science, 7:381, 1976.

Yellott, J.I., and P.R. Broadley. Fly Ash Separators for High Pressures and Temperatures. Ind. Eng. Chem. 47 (5): 944, 1955.